Calculations of nonlinear spectra of liquid Xe. II. Fifth-order Raman response

Jianshu Cao,[a] Shilong Yang, and Jianlan Wu
Department of Chemistry, Massachusetts Institute of Technology, Cambridge, Massachusetts 02139

(Received 11 July 2001; accepted 30 November 2001)

The polarization dependence and temporal profile of the fifth-order Raman response function and corresponding correlation function in liquid Xe are studied both analytically and numerically. Based on the symmetry of an isotropic sample, the fifth-order Raman response function has twelve distinct tensor elements, ten of which are independent, and the corresponding correlation function has twelve distinct tensor elements, seven of which are independent. The coefficients for decomposition into independent components are calculated explicitly based on the tensor property of an isotropic sample and are used to identify different coupling mechanisms in liquid Xe. The two-dimensional profile of the fifth-order Raman response function is evaluated by a simple hydrodynamic expression derived using the Gaussian factorization scheme. An alternative approach reduces the fifth-order Raman response function to time correlation functions that are easy to compute. [DOI: 10.1063/1.1445746]

I. INTRODUCTION

Ultrafast optical techniques open new possibilities for probing liquid dynamics.[1–7] One-dimensional time-domain experiments measure liquid motions in real time using techniques such as stimulated Raman scattering but have been shown to be equivalent to frequency domain linear absorption experiments.[8] In order to resolve the multiple time scales in liquids, Tanimura and Mukamel suggested fifth-order time-domain Raman spectroscopy, where liquid motions are perturbed by two pairs of Raman pulses separated by period t_1 of free induction and then probed after another period t_2.[9] The fifth-order off-resonant Raman measurement is an important example of two-dimensional optical spectroscopy, which is the analog of two-dimensional magnetic resonance. Two-dimensional spectroscopy holds the promise of monitoring the structural dynamics in liquids and thus resolving the mechanisms of line broadening observed in one-dimensional spectra.[10–19]

The relevant microscopic information for the fifth-order Raman experiment is described by the response function with two time variables t_1 and t_2,

$$R(t_2,t_1)=\langle\{\{\mathbf{\Pi}(t_2+t_1),\mathbf{\Pi}(t_1)\},\mathbf{\Pi}(0)\}\rangle$$
$$=-\beta\langle\{\mathbf{\Pi}(t_2+t_1),\mathbf{\Pi}(t_1)\}\dot{\mathbf{\Pi}}(0)\rangle, \qquad (1.1)$$

where β is the inverse temperature and $\{\ \}$ is the Poisson bracket. The total Raman polarizability $\mathbf{\Pi}$ is a second-rank tensor in three-dimensional Cartesian space, and the response function and the correlation function are sixth-rank tensors in three-dimensional Cartesian space. Unlike the linear response function discussed in the preceding paper[20] (hereafter referred to as Paper I) the response function cannot be expressed in terms of simple correlation functions. Appendix A includes three possible formulas for the fifth-order Raman response function by explicitly evaluating the Poisson bracket. These formulas involve the stability matrix, which may lead to divergence at sufficiently long times. This argument does not result in practical difficulties because the Boltzmann average cancels the classical divergence. Furthermore, the stability matrix in the nonlinear response function is associated with the interference effect among a pair of closely lying trajectories. Based on this observation, Mukamel pointed out that the nonlinear response can be a sensitive probe for classical chaos because sequences of multiple femtosecond pulses can be designed to directly probe the stability matrix.[21–23]

As a specific example to demonstrate some of these predictions, we recently explicitly calculated the linear and nonlinear response functions of a Morse oscillator based on the classical phase-space representation of the annihilation and creation operators.[24] Indeed, the classical response function for the Morse oscillator diverges linearly with time, whereas the quantum response function for a given eigen-energy is well defined for an eigenstate system. This classical divergence can be removed by phase-space averaging around the quantum eigen-energy surface and, interestingly, quantization of the phase space volume leads to the exact agreement between the averaged classical response function and the quantum response function. This analysis, along with earlier work,[25,26] confirms that thermal averaging removes the possible divergence caused by the stability matrix[22] and, to some degree, justifies the classical calculation of the nonlinear response of liquid Xe in this paper.

Third-order Raman spectroscopy in liquid Xe has been studied extensively in Paper I within the Drude oscillator model.[20] The Drude oscillator model consists of oscillating dipoles interacting through the second-order dipole tensor $\mathbf{T}$, which induces many-body polarization in liquids.[27–32] A brief description of the Drude oscillator model is presented in Appendix B for completeness, and the results from Paper

[a]Electronic mail: jianshu@mit.edu

I are summarized in the following. The Raman signal in rare gases arises from dipole–induced-dipole (DID) interactions. The leading contribution to the anisotropic component of the Raman spectrum is the two-body DID interaction, whereas the leading contribution to the isotropic component of the Raman spectrum is the three-body DID interaction. Higher order many-body polarization terms are incorporated through a renormalization procedure. In comparison with the anisotropic part, we find that the isotropic part of the effective dipole–dipole tensor has a short interaction range, resulting in a fast initial decay in the isotropic Raman response of atomic liquids. Polarization selectivity of third-order Raman spectroscopy is then studied within the Drude oscillator model. The third-order Raman response can be decomposed into an isotropic component and an anisotropic component with the coefficients determined uniquely by the tensor properties of the total polarizability. An interesting outcome of Paper I is the introduction of a simple mode coupling procedure: the Gaussian factorization scheme, which approximates liquid densities as Gaussian variables and maintains the equilibrium distribution by imposing pair correlation functions. In combination with the mean spherical approximation for the direct correlation function, we are able to recover the mode-coupling equation for the intermediate scattering function and the simple hydrodynamic expression for the third-order Raman correlation function. In comparison with the standard mode-coupling formalism, the Gaussian factorization scheme is direct and intuitive, and may help reveal underlying assumptions of mode-coupling theory. The scheme is used to evaluate the third-order Raman response in Paper I and the fifth-order Raman response in Sec. III of this paper.

A central issue of two-dimensional spectroscopy is the polarization dependence, which in principle allows us to selectively measure different types of interactions. The influence of the rotational Brownian motion on the fifth-order polarization was first examined by Tokmakoff with the implicit assumption of the equivalence between the polarization dependence of the response function and that of the correlation function.[33,34] The relative intensities at different geometries have also been estimated via the instantaneous normal mode (INM) method.[35–40] Kaufman, Blank, and Fleming[19] examined polarization selectivity in the fifth-order Raman signal of liquid CS_2 and found reasonable agreement with the INM predictions by Murry, Fourkas, and Keyes.[38–40] In Sec. II, the symmetry and polarization selectivity of the fifth-order Raman correlation function and response function are established without specific reference to the rotational Brownian model or the type of liquids. Within the renormalized Drude oscillator model, the twelve distinct tensor components are decomposed into independent components that correspond to different types of DID interactions and couplings in liquid Xe.

Multidimensional optical spectra have been successfully calculated using multilevel quantum dissipative systems or Brownian oscillator models. Mukamel's group used an oscillator picture to predict multidimensional spectroscopies of electronic and vibrational excitations.[41] Okumura and Tanimura developed a systematic expansion of the nonlinear response function of the dissipative anharmonic system.[42,43] Cho and co-workers derived expressions for various nonlinear Raman and infrared signals based on the system-bath Hamiltonian.[44,45] Since most liquids are classical at room temperature, we will calculate the fifth-order Raman response function in liquid Xe within classical mechanics. Although numerous theories and simulation methods have been developed for linear response processes,[46–52] relatively few attempts are made on the nonlinear response function. Molecular dynamics (MD) calculations of the third-order and fifth-order response functions have been carried out by Ma and Stratt on liquid Xe[53] and by Jansen, Snijders, and Duppen on CS_2.[54] These molecular dynamics simulations involve the propagation of the stability matrix or the actual simulation of the perturbed system on a time grid and are, therefore, computationally demanding. To avoid this difficulty, Mukamel, Piryatinski, and Chernyak explored semiclassical approximations for calculating multidimensional spectra in liquids.[55] Recently, Williams and Loring computed the classical mechanical vibrational echo by means of the fluctuating frequency approximation, which solves a driven dissipative anharmonic oscillator as a harmonic oscillator with a fluctuating frequency.[56,57] Denny and Reichman derived a mode-coupling expression for the fifth-order Raman signal in liquid Xe using a version of the quantum projection operator method and related the nonlinear response function to density fluctuations.[58] In Sec. III, we obtain a similar expression directly from classical mechanics without reference to quantum projection operators. Our approach is based on the Gaussian factorization scheme, which is shown in Paper I to recover the mode-coupling equation for the intermediate scattering function. The resulting expression for the fifth-order Raman response function compares well with numerical results and approximately reproduces the polarization dependence.

The difficulties in computing the fifth-order response function motivate us to seek a complementary approach. Instead of a direct calculation, the fifth-order response function is transformed in Sec. IV into the two-time correlation function or one-time correlation function. These correlation functions are easily examined for their time dependence and polarization dependence. As shown in Appendix A, the fifth-order Raman response function cannot be written as a correlation function without involving the stability matrix; thus certain information content in the response function is lost upon transformation. Nevertheless, these correlation functions can be calculated and analyzed accurately, thus providing a different perspective of two-dimensional Raman spectroscopy.

II. POLARIZATION SELECTIVITY

A. Symmetry and independent components

To explore the symmetry of the fifth-order Raman response function, we first study the two-time correlation function for the total polarizability, defined as

$$C(t_2,t_1)=\langle \mathbf{\Pi}(t_2+t_1)\mathbf{\Pi}(t_1)\mathbf{\Pi}(0)\rangle \tag{2.1}$$

whose relationship to the fifth-order Raman response function is explained in Appendix A. The two-time correlation

TABLE I. Decomposition of the twelve distinct tensor elements of the fifth-order Raman correlation function into five independent components, as defined via the reduced probability distribution function in Sec. II B.

	$C(t_2,t_1)$	$\langle DDD\rangle$	$\langle IDD\rangle$	$\langle DID\rangle$	$\langle DDI\rangle$	$\langle III\rangle$
C_1	*ZZZZZZ*	16/35	4/5	4/5	4/5	1
C_2	*YYZZZZ*	−8/35	4/5	−2/5	−2/5	1
C_3	*ZZYYZZ*	−8/35	−2/5	4/5	−2/5	1
C_4	*ZZZZYY*	−8/35	−2/5	−2/5	4/5	1
C_5	*ZZYYXX*	16/35	−2/5	−2/5	−2/5	1
C_6	*ZZZYZY*	6/35	1/5	0	0	0
C_7	*ZYZZZY*	6/35	0	1/5	0	0
C_8	*ZYZYZZ*	6/35	0	0	1/5	0
C_9	*ZZXYXY*	−12/35	1/5	0	0	0
C_{10}	*XYZZXY*	−12/35	0	1/5	0	0
C_{11}	*XYXYZZ*	−12/35	0	0	1/5	0
C_{12}	*ZYYXXZ*	9/35	0	0	0	0

function is a six-rank tensor with $3^6=726$ tensor elements. In an isotropic sample, the symmetry of reflection in any plane removes all elements with an odd number of any Cartesian index and leaves 183 tensor elements.[59] Further, the correlation function is invariant to the permutation of the Cartesian coordinate and the interchange of indices of a Raman pulse pair. Thus, the two-time correlation function tensor for the total polarizability consists of twelve distinct elements, which will be calculated explicitly in this section.

To proceed, we construct three combinations of correlation functions from the tensor elements:

$$Z_\mu = C_{\mu\mu\mu\mu\mu\mu} \tag{2.2}$$

with one distinct Cartesian index,

$$Z_{\mu\nu} = C_{\nu\nu\mu\mu\mu\mu} + C_{\mu\mu\nu\nu\mu\mu} + C_{\mu\mu\mu\mu\nu\nu} + 4(C_{\mu\mu\mu\nu\mu\nu} + C_{\mu\nu\mu\mu\mu\nu} + C_{\mu\nu\mu\nu\mu\mu}) \tag{2.3}$$

with two distinct Cartesian indices, and

$$Z_{\mu\nu\gamma} = C_{\mu\mu\nu\nu\gamma\gamma} + 2(C_{\gamma\gamma\mu\nu\mu\nu} + C_{\mu\nu\gamma\gamma\mu\nu} + C_{\mu\nu\mu\nu\gamma\gamma}) + 8C_{\mu\nu\nu\gamma\gamma\mu} \tag{2.4}$$

with three distinct Cartesian indices. The coefficients in the above-presented equations arise from the accounting due to the interchange of the indices in each pairs of Raman pulses. The permutation of the Cartesian coordinate makes all members in each set equivalent. For an isotropic sample, rotation along any axis will not change the value of the matrix element. As derived in Appendix C, the rotational symmetry introduces rigorous ratios among the three sets:

$$Z_\mu : Z_{\mu\nu} : Z_{\mu\nu\gamma} = 1:3:1 \tag{2.5}$$

leaving ten independent components for the two-time correlation function.

Finally, the time reversal symmetry of the equilibrium liquid allows us to write

$$C_{\mu_2\nu_2\mu_1\nu_1\mu_0\nu_0}(t_2,t_1) = C_{\mu_0\nu_0\mu_1\nu_1\mu_2\nu_2}(t_1,t_2), \tag{2.6}$$

where both the two time variables and the two corresponding pairs of electric field polarizations are interchanged. Explicitly, from the twelve tensor elements in Table I, we have $C_{yyzzzz}(t_2,t_1)=C_{zzzzyy}(t_1,t_2)$, $C_{zzzyzy}(t_2,t_1)=C_{zyzyzz}\times(t_1,t_2)$, and $C_{zzxyxy}(t_2,t_1)=C_{xyxyzz}(t_1,t_2)$, thus removing three independent components. In conclusion, with all the symmetry considerations, the number of independent polarization components for the two-time correlation function is seven.

The tensor symmetry in the two-time correlation function gives more polarization selectivity than that in the single-time correlation function and can be used to extract more information about internuclear interactions in liquids. As shown in Paper I, the correlation function in the third-order Raman experiment is a fourth-rank tensor and has two independent components. Interestingly, the normalized dipole–dipole interaction model has an isotropic component and an anisotropic component, which can be separated in the third-order experiment. But, additional components, such as the contribution of the nonresonant scattering and the deviation from the DID interaction, cannot be isolated in the third-order measurement. The seven independent components in the two-time correlation function provide the potential to isolate more independent contributions to the Raman signal.

B. Reduced probability distribution

Within the renormalized DID approximation, the two-time correlation function can be written in a general form as

$$C(t_2,t_1) = \langle \mathbf{\Pi}(t_2+t_1)\mathbf{\Pi}(t_1)\mathbf{\Pi}(0)\rangle = \overline{\alpha}^6 \int d\mathbf{r}_0\, d\mathbf{r}_1\, d\mathbf{r}_2\, \overline{\mathbf{T}}(\mathbf{r}_2)\overline{\mathbf{T}}(\mathbf{r}_1)\overline{\mathbf{T}}(\mathbf{r}_0) \times P(\mathbf{r}_0,0;\mathbf{r}_1,t_1;\mathbf{r}_2,t_1+t_2), \tag{2.7}$$

where $P(\mathbf{r}_0,0;\mathbf{r}_1,t_1;\mathbf{r}_2,t_1+t_2)$ is the reduced joint probability distribution function (PDF) for finding one pair of liquid particles with relative coordinate $\mathbf{r}_0$ at zero time, one pair of liquid particles with relative coordinate $\mathbf{r}_1$ at time t_1, and one pair of liquid particles with relative coordinate $\mathbf{r}_2$ at time t_2. The reduced probability is obtained after integrating all other degrees of freedom except for $\mathbf{r}_0$, $\mathbf{r}_1$, and $\mathbf{r}_2$.

For an isotropic liquid, the joint probability distribution function is a function of the relative positions and the relative angles

$$P(\mathbf{r}_0,0;\mathbf{r}_1,t_1;\mathbf{r}_2,t_1+t_2) = P(r_0,r_1,r_2,\hat{\mathbf{r}}_{01},\hat{\mathbf{r}}_{12},\hat{\mathbf{r}}_{20},0,t_1,t_1+t_2), \tag{2.8}$$

where $\hat{\mathbf{r}}_{01}$ is the angle formed by unit vectors $\hat{r}_1$ and $\hat{r}_1$, $\hat{\mathbf{r}}_{12}$ and $\hat{\mathbf{r}}_{20}$ are defined in a similar fashion. With a relatively large temporal separation of (t_2-t_1), the angular correlation between the first pair and the last pair is weak so that

$$P(\mathbf{r}_0,0;\mathbf{r}_1,t_1;\mathbf{r}_2,t_1+t_2)\approx P(r_0,r_1,r_2,\hat{\mathbf{r}}_{01},\hat{\mathbf{r}}_{12},0,t_1,t_1+t_2), \tag{2.9}$$

where the functional dependence on $\hat{\mathbf{r}}_{02}$ is ignored. Then, the approximate PDF can be expanded as a function of the angle between $\mathbf{r}_2$ and $\mathbf{r}_1$ and the angle between $\mathbf{r}_1$ and $\mathbf{r}_0$, giving

$$\begin{aligned}P(\mathbf{r}_0,0;\mathbf{r}_1,t_1;\mathbf{r}_2,t_1+t_2)&\approx\frac{1}{4\pi}\sum_{lm}Y_{lm}(\hat{\mathbf{r}}_0)Y^*_{lm}(\hat{\mathbf{r}}_1)\,\frac{1}{4\pi}\sum_{l'm'}Y_{l'm'}(\hat{\mathbf{r}}_1)Y^*_{l'm'}(\hat{\mathbf{r}}_2)\\&\quad\times P_{ll'}(r_0,0;r_1,t_1;r_2,t_1+t_2),\end{aligned} \tag{2.10}$$

where Y_{lm} is the spherical harmonic function. Substituting Eq. (2.10) into Eq. (2.7) and separating the angular and radial parts of the spatial integration, we have

$$\begin{aligned}C(t_2,t_1)\approx&\langle\mathbf{D}_{\mu_2\nu_2}\mathbf{D}_{\mu_1\nu_1}\mathbf{D}_{\mu_0\nu_0}\rangle C_{DDD}(t_2,t_1)\\&+\langle\mathbf{D}_{\mu_2\nu_2}\mathbf{D}_{\mu_1\nu_1}\mathbf{I}_{\mu_0\nu_0}\rangle C_{DDI}(t_2,t_1)\\&+\langle\mathbf{D}_{\mu_2\nu_2}\mathbf{I}_{\mu_1\nu_1}\mathbf{D}_{\mu_0\nu_0}\rangle C_{DID}(t_2,t_1)\\&+\langle\mathbf{I}_{\mu_2\nu_2}\mathbf{D}_{\mu_1\nu_1}\mathbf{D}_{\mu_0\nu_0}\rangle C_{IDD}(t_2,t_1)\\&+\langle\mathbf{I}_{\mu_2\nu_2}\mathbf{I}_{\mu_1\nu_1}\mathbf{I}_{\mu_0\nu_0}\rangle C_{III}(t_2,t_1),\end{aligned} \tag{2.11}$$

where the orientational average is taken with respect to the angles between unit vectors. The first term is the contribution from the anisotropic polarizability, the last term from the isotropic polarizability, and the three other terms are the mixed contributions. The radial parts are time dependent and are given explicitly as

$$\begin{aligned}C_{DDD}(t_2,t_1)&=\overline{\alpha}^6\int d\mathbf{r}_0\,d\mathbf{r}_1\,d\mathbf{r}_2\,P_{22}(r_0,0;r_1,t_1;r_2,t_1+t_2)h_D(r_0)h_D(r_1)h_D(r_2),\\C_{IDD}(t_2,t_1)&=\overline{\alpha}^6\int d\mathbf{r}_0\,d\mathbf{r}_1\,d\mathbf{r}_2\,P_{02}(r_0,0;r_1,t_1;r_2,t_1+t_2)h_I(r_0)h_D(r_1)h_D(r_2),\\C_{DID}(t_2,t_1)&=\overline{\alpha}^6\int d\mathbf{r}_0\,d\mathbf{r}_1\,d\mathbf{r}_2\,P_{22}(r_0,0;r_1,t_1;r_2,t_1+t_2)h_D(r_0)h_I(r_1)h_D(r_2),\\C_{DDI}(t_2,t_1)&=\overline{\alpha}^6\int d\mathbf{r}_0\,d\mathbf{r}_1\,d\mathbf{r}_2\,P_{20}(r_0,0;r_1,t_1;r_2,t_1+t_2)h_D(r_0)h_D(r_1)h_I(r_2),\\C_{III}(t_2,t_1)&=\overline{\alpha}^6\int d\mathbf{r}_0\,d\mathbf{r}_1\,d\mathbf{r}_2\,P_{00}(r_0,0;r_1,t_1;r_2,t_1+t_2)h_I(r_0)h_I(r_1)h_I(r_2),\end{aligned} \tag{2.12}$$

which can also be expressed in terms of the Legendre polynomial as a function of the time-dependent angles. Clearly, the relationship $C_{IDD}(t_2,t_1)=C_{DDI}(t_1,t_2)$ vindicates the time reversal symmetry and leaves effectively four independent radial functions. The angular average, which defines the coefficients in the decomposition, is expressed explicitly as

$$\begin{aligned}&\langle\mathbf{D}_{zz}\mathbf{D}_{zz}\mathbf{D}_{zz}\rangle\\&\quad=\frac{1}{4\pi}\int d\hat{\mathbf{r}}_2\,d\hat{\mathbf{r}}_1\,d\hat{\mathbf{r}}_0\,\mathbf{D}_{zz}(\hat{\mathbf{r}}_2)\mathbf{D}_{zz}(\hat{\mathbf{r}}_1)\mathbf{D}_{zz}(\hat{\mathbf{r}}_0)\\&\qquad\times\sum_m Y_{2m}(\hat{\mathbf{r}}_0)Y^*_{2m}(\hat{\mathbf{r}}_1)\sum_{m'}Y_{2m'}(\hat{\mathbf{r}}_1)Y^*_{2m'}(\hat{\mathbf{r}}_2)\\&\quad=\frac{1}{4\pi}\int d\hat{\mathbf{r}}\,\mathbf{D}_{zz}(\hat{\mathbf{r}})\mathbf{D}_{zz}(\hat{\mathbf{r}})\mathbf{D}_{zz}(\hat{\mathbf{r}})\\&\quad=\frac{16}{35}\end{aligned} \tag{2.13}$$

and similarly for other angular averages. In Table I, these coefficients are explicitly evaluated for all twelve tensor elements and can be verified for their rotational symmetry and time reversal symmetry. The ratios listed in Table I are similar to those derived from the rotational diffusion model of the dipolar fluid[34] or those evaluated through the normal mode analysis.[40] The derivation and the symmetry analysis here and hereafter are more general and rigorous.

A key consideration is that for atomic fluids the dipole is formed transiently by at least two atoms. To leading order, two atoms form a transient molecule bond through the dipole–induced-dipole interaction and give rise to the anisotropic polarizability, whereas the three-body polarization effect leads to the isotropic polarizability and additional atomic polarizability. Therefore, to leading order, the transient anisotropic polarizability is independent of the liquid density, whereas the isotropic polarizability is proportional to the liquid density. As a result, the anisotropic part of the polarization tensor is larger than the isotropic part, and we estimate the relative intensity for the radial function as $C_{DDD}>C_{IDD}$, C_{DID}, $C_{DDI}>C_{III}$. In a dilute sample, we have only the depolarization polarizability with the resulting time dependence given by $C_{DDD}(t_2,t_1)$, so that the intensity of the tensor element follows the ratios indicated by the first column in Table I. As the liquid density increases, these ratios will be contaminated by the contribution from the isotropic part of the DID polarizability and will be modified according to Eq. (2.11).

The diffusion model is used in Paper I for the third-order Raman correlation function to demonstrate a slow free induction decay for the isotropic component and a fast free induction decay for the depolarized component. The asymptotic behavior of each independent component in Eq. (2.11) approaches exponential decay with a decay constant λ. This argument predicts λ_{DDD}, $\lambda_{DID}>\lambda_{DDI}$, $\lambda_{IDD}>\lambda_{III}$, where the subscripts denote the five components. Though obtained for the two-time correlation function, these predictions also apply to the fifth-order Raman response function in the long-time limit.

TABLE II. Decomposition of the fifth-order Raman response function and correlation function into five independent components based on symmetry considerations. The coefficients are normalized by the $ZZZZZZ$ component, with two undetermined difference coefficients $\delta c_6 \neq \delta c_8$ for the response function, and with one undetermined difference coefficient $\delta c = \delta c_6 = \delta c_8$ for the correlation function.

	$C(t_1,t_2)$	c_{DDD}	c_{IDD}	c_{DID}	c_{DDI}	c_{III}
C_1	$ZZZZZZ$	1	1	1	1	1
C_2	$YYZZZZ$	$-1/2$	1	$-1/2$	$-1/2$	1
C_3	$ZZYYZZ$	$-1/2$	$-1/2$	1	$-1/2$	1
C_4	$ZZZZYY$	$-1/2$	$-1/2$	$-1/2$	1	1
C_5	$ZZYYXX$	1	$-1/2$	$-1/2$	$-1/2$	1
C_6	$ZZZYZY$	$3/8-\delta c_6$	1/4	0	0	0
C_7	$ZYZZZY$	$3/8+\delta c_6+\delta c_8$	0	1/4	0	0
C_8	$ZYZYZZ$	$3/8-\delta c_8$	0	0	1/4	0
C_9	$ZZXYXY$	$-3/4-2\delta c_6$	1/4	0	0	0
C_{10}	$XYZZXY$	$-3/4+2\delta c_6+2\delta c_8$	0	1/4	0	0
C_{11}	$XYXYZZ$	$-3/4-2\delta c_8$	0	0	1/4	0
C_{12}	$ZYYXXZ$	9/16	0	0	0	0

C. General polarization selectivity of the correlation function

The ratios in Table I are valid both in the initial time regime and in the long-time regime. It is reasonable to speculate that these ratios are more general than demonstrated through the approximate RDF in Sec. II C. Indeed, a set of ratios similar to Table I can be established more generally based on the tensor property of the total polarizability and the symmetry of an isotropic sample.

Within the Drude oscillator model, the total polarizability for an isotropic sample is written as $\mathbf{\Pi}=\mathbf{\Pi}_I+\mathbf{\Pi}_D$, where $\mathrm{Tr}\,\mathbf{\Pi}_D=0$ is the anisotropic part and $\mathbf{\Pi}_I \propto \mathbf{I}$ is the isotropic part. Then, the two-time correlation function can be decomposed as

$$\begin{aligned} C(t_2,t_1) = & c_{DDD}C_{DDD}(t_2,t_1)+c_{IDD}C_{IDD}(t_2,t_1) \\ & +c_{DID}C_{DID}(t_2,t_1)+c_{DDI}C_{DDI}(t_2,t_1) \\ & +c_{III}C_{III}(t_2,t_1), \end{aligned} \tag{2.14}$$

where components such as C_{DII}, C_{IDI}, and C_{IID} vanish because of the symmetry of the $\mathbf{D}$ tensor. The time-reversal symmetry requires $C_{IDD}(t_2,t_1)=C_{DDI}(t_1,t_2)$, effectively reducing the number of independent components to four. Here, $C_{DDD}(t_2,t_1)$ is the component associated with $\langle \mathbf{\Pi}_D(t_2+t_1)\mathbf{\Pi}_D(t_1)\mathbf{\Pi}_D(0)\rangle$ with the corresponding coefficient given by c_{DDD}, and similar definitions hold for the other terms.

The coefficient depends on the polarization geometry. As an example, we evaluate c_{DDD} explicitly. From the zero-trace definition of the $\mathbf{\Pi}_D$ tensor, we have

$$C_{zzzzzz}+C_{yyzzzzz}+C_{xxzzzz}=0 \tag{2.15}$$

so that $c_1=-2c_2=\xi_1$ with ξ_1 the value of c_1. Here, the index of the coefficient follows the definition in Table I. Similarly, we have $c_3=c_4=-(1/2)\xi_1$ and $c_5=\xi_1$, and thus obtain the rigorous ratios for the group of the first five coefficients. The second group consists of the coefficients from c_6 to c_{11}. The zero-trace identity leads to

$$C_{zzzyzy}+C_{yyzyzy}+C_{xxzyzy}=0, \tag{2.16}$$

yielding $c_9=-2c_6$, and similarly we have $c_{10}=-2c_7$ and $c_{11}=-2c_8$. In addition, the time-reversal symmetry gives $c_6=c_8$ and $c_9=c_{11}$. For simplicity, we define an average coefficient as $\xi_2=(2c_6+c_7)/3$ to represent the second group. Together, the twelve distinct tensor elements are reduced to the three independent coefficients associated with the three groups: ξ_1, ξ_2, and ξ_3, where $\xi_3=c_{12}$. These coefficients are related to each other through the two conditions in Eq. (2.5) imposed by rotational symmetry. The first condition $Z_{\mu\nu}=3Z_\mu$ becomes

$$3c_1=c_2+c_3+c_4+4(c_6+c_7+c_8), \tag{2.17}$$

which predicts $\xi_1:\xi_2=8:3$, and the second condition $Z_{\mu\nu\gamma}=Z_\mu$ becomes

$$c_1=c_5+2(c_9+c_{10}+c_{11})+8c_{12}, \tag{2.18}$$

which predicts $\xi_1:\xi_3=16:9$. Hence, the ratios for the twelve coefficients associated with the $C_{DDD}(t_2,t_1)$ component can be rigorously obtained from the symmetry arguments. Similarly, the ratios for other components can be obtained and are listed in Table II. These ratios are the same as those derived from the angular average in Table I of Sec. II B, except for the undetermined difference coefficient δc between c_6 and c_8. Therefore, the symmetry relations alone determine the decomposition into various components and the relative ratios.

In general, the fifth-order Raman response function does not follow the polarization dependence derived here for the two-time correlation function. However, if the rotational motion is much slower than the vibrational motion, the Poisson bracket applies to the vibrational degrees of freedom but not to the rotational degrees of freedom, so that the fifth-order Raman response function follows the same polarization selectivity as described here for the two-time correlation function. This argument may be useful for establishing the polarization selectivity of multipulse infrared spectroscopy.

D. General polarization selectivity of the response function

In Secs. II A–II C, we discussed the polarization dependence of the two-time correlation function associated with the fifth-order response function. As will be seen in the following, the polarization dependence of the fifth-order response function is similar but with some additional subtleties. Following the arguments in Sec. II A, the fifth-order Raman response function is a six-rank tensor, with 726 elements. In an isotropic sample, the permutation of the Cartesian axis and the interchange of the indices for a pair of Raman pulses leave twelve distinct tensor elements, as listed in Table I. For the response function, $R(t_2,t_1)=-\beta\langle\{\mathbf{\Pi}(t_2+t_1),\mathbf{\Pi}(t_1)\}\dot{\mathbf{\Pi}}(0)\rangle$, the time-derivative $\dot{\mathbf{\Pi}}$ obeys the same rotational transformation as the total polarizability tensor, and the Poisson bracket, $\{\mathbf{\Pi}(t_2+t_1),\mathbf{\Pi}(t_1)\}$, as a whole also preserves the same rotational symmetry as the product $\mathbf{\Pi}(t_2+t_1)\mathbf{\Pi}(t_1)$. The rotational symmetry of the isotropic sample imposes the same ratios among the three combinations of the response function as Eq. (2.5). However, unlike the correlation function in Sec. II A, the response function does not follow the time-reversal symmetry, as the two time variables t_1 and t_2 are not equivalent in Eq. (1.1). Therefore, the twelve distinct tensor elements have ten independent components for the fifth-order Raman response function, in contrast to seven independent components for the fifth-order Raman correlation function.

Since the explicit expressions for the fifth-order Raman response function involve the momentum and the stability matrix, we cannot adopt the polarization analysis based on the reduced probability distribution in Sec. II B. Fortunately, the more general analysis in Sec. II C still holds for the response function. Within the Drude oscillator model, we decompose the response function as

$$\begin{aligned}R(t_2,t_1)=&c_{DDD}R_{DDD}(t_2,t_1)+c_{IDD}R_{IDD}(t_2,t_1)\\&+c_{DID}R_{DID}(t_2,t_1)+c_{DDI}R_{DDI}(t_2,t_1)\\&+c_{III}R_{III}(t_2,t_1),\end{aligned}\tag{2.19}$$

where components such as R_{DII}, R_{IDI}, and R_{IID} vanish because of the symmetry of the $\mathbf{D}$ tensor. In Eq. (2.19), $R_{DDD}(t_2,t_1)$ is the component associated with $\langle\{\{\mathbf{\Pi}_D(t_2+t_1),\mathbf{\Pi}_D(t_1)\},\mathbf{\Pi}_D(0)\}\rangle$ with the corresponding coefficient given by $C_{DDD}(t_2,t_1)$, and similar definitions hold for the other terms. To determine these coefficients, we use the same symmetry arguments as in Sec. II C and find the same ratios as in Table I except for c_{DDD}. The lack of the time reversal symmetry for the response function removes the equality between $c_{6,DDD}$ and $c_{8,DDD}$ and between $c_{9,DDD}$ and $c_{11,DDD}$. Nevertheless, we can still define the average coefficient for the second group as $\xi=(c_6+c_7+c_8)/3$, which is determined through the rotational symmetry relations. These coefficients for the response function, listed in Table II, differ from those for the correlation function in that $\delta c_6\neq\delta c_8$.

The five independent components in Eq. (2.19) measure microscopic couplings in liquids and their time evolution. For example, $R_{DDD}(t_2,t_1)$ describes the depolarized Raman signal as a consequence of the vibration motions induced by two depolarized Raman interactions at zero time and at time t_1, respectively. R_{IDD} describes the isotropic Raman signal as a consequence of the vibration motions induced by two depolarized Raman interactions at zero time and at time t_1, respectively. R_{DID} describes the depolarized Raman signal as a consequence of the vibration motions induced by one depolarized Raman interaction at zero time and another isotropic Raman interaction at time t_1. The two other components R_{DDI} and R_{III} can be understood in a similar way.

Since the third-order polarization has two independent components, the third-order experiment cannot be used to isolate the contribution of the nonresonant scattering or the deviation from the DID interaction. Within the renormalized Drude oscillator model, the fifth-order Raman spectrum consists of five independent components though ten components are allowed by the symmetry considerations. Thus, the additional components can be used to identify other contributions which cannot be isolated in the third-order Raman experiment.

E. A numerical example

We calculated the fifth-order Raman correlation function using molecular dynamics simulation of a box of 108 Xe atoms at reduced temperature $T^*=0.76$ and reduced density $\rho^*=0.85$. The simulation details, the Lennard-Jones parameters for liquid Xe, and other relevant parameters can be found in Paper I. Since the contribution from the isotropic polarizability is relatively weak for liquid Xe (about 10% for the thermodynamic state), we adopted the first-order pair-interaction approximation of the polarization tensor, $\mathbf{\Pi}=\Sigma\alpha\mathbf{T}\alpha$, to study the anisotropic contribution. The spherical cutoff at half the box size was used to facilitate the simulation so that long MD trajectories can be obtained with reasonable amount of CPU time. As shown in Sec. II A, the two-time correlation function has twelve distinct tensor elements due to the reflection symmetry and Kleinmann symmetry. These tensor elements follow the ratios given in the first column of Table I, or the first column of Table II. The latter ratios are determined by the rotational isotropic condition and the traceless property of the total polarizability tensor and are thus more rigorous. In our calculation, the reference frame is randomly rotated to enforce the isotropic condition and minimize the orientational preference.

As shown in Fig. 1, the twelve tensor elements of $C(0,t)$ follow the ratios given in Table I of Sec. II B consistently over the entire time scale. On careful examination, we notice the slight difference between $C_6=C_8$ and C_7 as well as between $C_9=C_{11}$ and C_{10}. This observation is consistent with the general polarization dependence derived in Sec. II C and listed in Table II, where the difference coefficient $\delta c=\delta c_6=\delta c_8$ is responsible for the observed difference. In Fig. 2, the twelve tensor elements, normalized by the ratios in the first column of Table I, all fall onto the same curve within numerical error. This master curve is the anisotropic part of the correlation function $C_{DDD}(t_2,t_1)$. The diagonal cross sections of the twelve tensor elements, $C(t,t)$, are plotted in Fig. 3, and are found to obey the same ratios as listed in Table II. The two-dimensional contour $C_{zzzzzz}(t_1,t_2)$ in Fig. 4 demonstrates the basic features of the two-time correlation

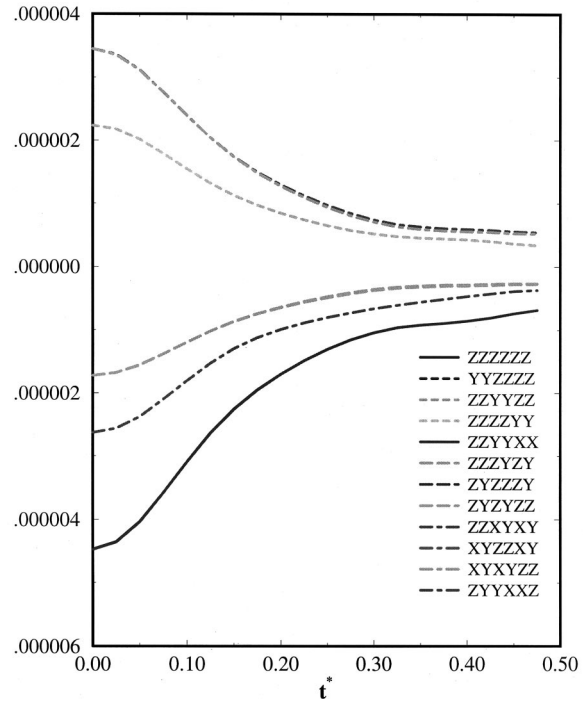

FIG. 1. Twelve components of the fifth-order Raman correlation function along the time axis $C(t,0)$. The molecular dynamics simulation was carried out for a simulation box of 108 Xe atoms at reduced temperature $T^*=0.76$ and reduced density $\rho^*=0.85$.

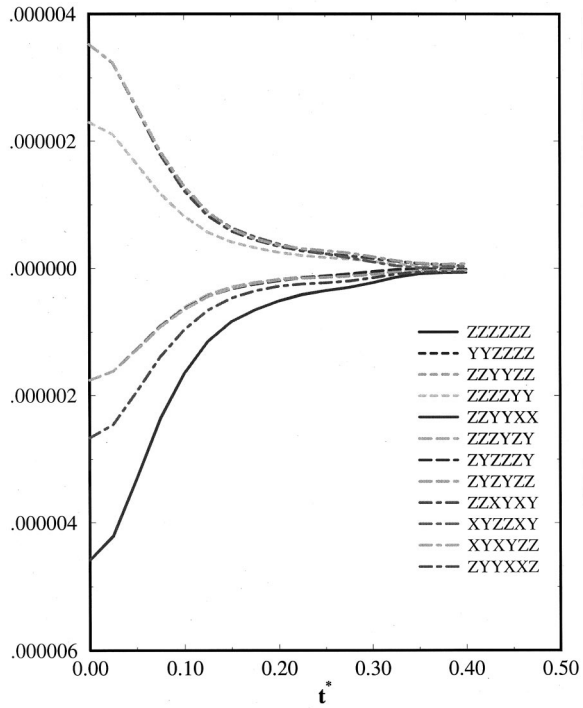

FIG. 3. Twelve components of the diagonal element of the fifth-order Raman correlation function $C(t,t)$, obtained from the same simulation as in Fig. 1.

function. The sparse contour lines at $t\leqslant 0.05$ and $t\geqslant 0.25$ indicate slow variations in both in the short-time regime and in the long time regime, while the dense contour lines indicate the fast decay in the intermediate time regime. These features are consistent with our observations in Figs. 1 and 3.

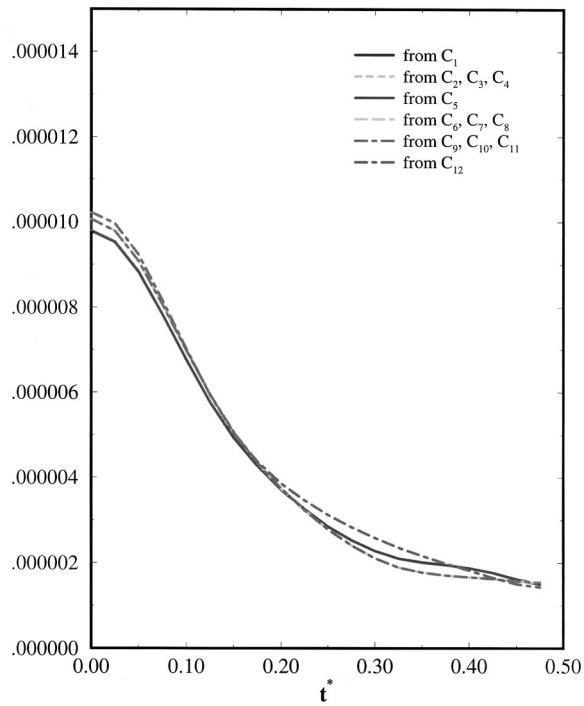

FIG. 2. Twelve components of the correlation function $C(0,t)$ in Fig. 1 normalized by the coefficients in the first column of Table I.

III. HYDRODYNAMIC EVALUATION: GAUSSIAN FACTORIZATION

In the long time-scale and length-scale limit, density fluctuations in simple liquids are usually described as a stochastic Gaussian process so that multiple time and multiple point correlation function can be decomposed to correlation functions of linear hydrodynamic modes. Specifically, the

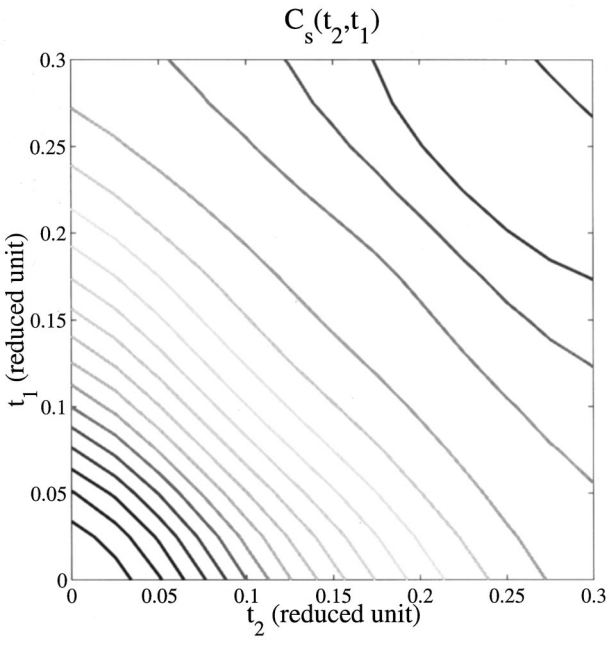

FIG. 4. A two-dimensional contour plot of $C_{zzzzzz}(t_2,t_1)$, obtained from the same simulation as in Fig. 1.

Gaussian factorization scheme combined with the mean spherical approximation for the direct pair correlation function allows us to obtain the standard mode coupling equation for the intermediate scattering function.[20] Here, we explicitly include the Poisson brackets in the Gaussian factorization of the fifth-order response function.

It is a standard procedure to express the polarizability tensor in Fourier space as

$$\Pi=\sum_{i\neq j}\bar{\alpha}\bar{\mathbf{T}}_{ij}\bar{\alpha}=\frac{\bar{\alpha}^2}{V}\sum_{\mathbf{k}}\bar{\mathbf{T}}(\mathbf{k})\sum_{ij}e^{i\mathbf{k}(\mathbf{r}_i-\mathbf{r}_j)}$$
$$=\frac{\bar{\alpha}^2}{V}\sum_{\mathbf{k}}\bar{\mathbf{T}}(\mathbf{k})\rho(\mathbf{k})\rho^*(\mathbf{k}), \tag{3.1}$$

where $\rho(\mathbf{k})=\Sigma_i\exp(-i\mathbf{k}\mathbf{r}_i)$ is the number density, and the term with $i=j$ is excluded by setting the dipole interaction to zero whenever the internuclear distance vanishes. We expand the response function in Fourier space,

$$R(t_2,t_1)=-\beta\frac{\partial}{\partial t_1}\langle\{\mathbf{\Pi}(t_2+t_1),\mathbf{\Pi}(t_1)\}\mathbf{\Pi}(0)\rangle$$
$$=\left(\frac{\bar{\alpha}^2}{V}\right)^3\beta\frac{\partial}{\partial t_1}\sum_{\mathbf{k}_2}\sum_{\mathbf{k}_1}\sum_{\mathbf{k}}\bar{\mathbf{T}}(\mathbf{k}_2)\bar{\mathbf{T}}(\mathbf{k}_1)\bar{\mathbf{T}}(\mathbf{k})$$
$$\times\langle\{\rho_2\rho_2^*,\rho_1\rho_1^*\}\rho_0\rho_0^*\rangle, \tag{3.2}$$

where $\rho_2=\rho(\mathbf{k}_2,t_2)$, $\rho_1=\rho(\mathbf{k}_1,t_1)$, and $\rho_0=\rho(\mathbf{k},t_0)$, and ρ^* is the complex conjugate of the density operator. The Poisson bracket of the bilinear density terms in the polarizability tensor is expanded as

$$\{\rho_2\rho_2^*,\rho_1\rho_1^*\}=\rho_2\{\rho_2^*,\rho_1\}\rho_1^*+\rho_2\{\rho_2^*,\rho_1^*\}\rho_1$$
$$+\rho_2^*\{\rho_2,\rho_1\}\rho_1^*+\rho_2^*\{\rho_2,\rho_1^*\}\rho_1. \tag{3.3}$$

Applying the Gaussian factorization scheme to the first term in Eq. (3.3) gives

$$\bar{\mathbf{T}}(\mathbf{k}_2)\bar{\mathbf{T}}(\mathbf{k}_1)\bar{\mathbf{T}}(\mathbf{k})\langle\rho_2\{\rho_2^*,\rho_1\}\rho_1^*\rho_0\rho_0^*\rangle$$
$$\approx\delta_{\mathbf{k}_1,\mathbf{k}}\delta_{\mathbf{k}_2,\mathbf{k}}\bar{\mathbf{T}}_g(\mathbf{k})\bar{\mathbf{T}}_g(\mathbf{k})\bar{\mathbf{T}}_g(\mathbf{k})\langle\{\rho_2^*,\rho_1\}\rangle\langle\rho_2\rho_0^*\rangle\langle\rho_1^*\rho_0\rangle$$
$$=N^3\delta_{\mathbf{k}_1,\mathbf{k}}\delta_{\mathbf{k}_2,\mathbf{k}}\bar{\mathbf{T}}_g(\mathbf{k})\bar{\mathbf{T}}_g(\mathbf{k})\bar{\mathbf{T}}_g(\mathbf{k})\beta\dot{F}(\mathbf{k},t_2)$$
$$\times F(\mathbf{k},t_2+t_1)F(\mathbf{k},t_1), \tag{3.4}$$

where the dipole propagator $\bar{\mathbf{T}}$ is changed into the dressed dipole propagator $\bar{\mathbf{T}}_g(\mathbf{r})=\bar{\mathbf{T}}(\mathbf{r})g(r)$ upon decomposition. Other ways of factorizing density operators lead to a single left or right Poisson bracket in the ensemble average and thus do not contribute to the response function. It can be confirmed that the other three terms in Eq. (3.3) give the same result as Eq. (3.4). Combining Eq. (3.2) with Eq. (3.3), we arrive at

$$R(t_2,t_1)\approx 4N\rho^2\beta^2\bar{\alpha}^6\frac{1}{(2\pi)^3}$$
$$\times\int d\mathbf{k}\,\bar{\mathbf{T}}_g(\mathbf{k})\bar{\mathbf{T}}_g(\mathbf{k})\bar{\mathbf{T}}_g(\mathbf{k})\frac{\partial}{\partial t_2}F(\mathbf{k},t_2)\frac{\partial}{\partial t_1}$$
$$\times[F(\mathbf{k},t_2+t_1)F(\mathbf{k},t_1)], \tag{3.5}$$

where $\bar{\mathbf{T}}_g$ should be understood as the tensor element with the indices specified by the response function. The simple Gaussian factorization scheme decomposes the fifth-order Raman response function into product of correlation functions, thus relating the fifth-order Raman signal to density fluctuations in atomic liquids. This relation was first demonstrated by Denny and Reichman, and we refer to their letter[58] for further discussions on its physical implications.

As mentioned in Sec. I, our Gaussian factorization expression in Eq. (3.5) is similar to the original mode coupling expression derived by Denny and Reichman from a version of the quantum projection operator method.[58] In fact, the time-dependent parts in the Fourier integrand are the same, whereas the static parts are different because the Gaussian factorization scheme does not directly involve the projection onto bilinear modes. Since the Poisson bracket is the classical limit of the quantum commutator, the classical response function is well defined and can be evaluated directly via classical mode coupling theory without taking the classical limit of quantum mode coupling theory. To demonstrate this point, we rederive Eq. (3.5) in Appendix D by applying the Gaussian factorization scheme to quantum operators and then taking the classical limit.

The simple correlation function form in Eq. (3.5) makes it possible to analyze polarization selectivity in a similar fashion as the two-time correlation function in Sec. II B. For isotropic liquids, the renormalized DID model reduces the twelve tensor elements for the response function in Eq. (3.5) into four independent components. In Eq. (3.5), the fifth-order Raman response function is factorized into the angular part and the radial part, so that the decomposition coefficients can be computed from the angular integration and are given by the first column of Table I. However, as analyzed in Sec. II C, this simple decomposition procedure does not hold rigorously for the the fifth-order response function, because the decomposition coefficients are modified by δc_8 and δc_6. Though the simple Gaussian factorization approach gives a reasonable temporal profile in the intermediate time regime, its prediction of polarization selectivity is not rigorous and its prediction of short-time behaviors is not reliable. These difficulties are not surprising because the Gaussian factorization scheme is not valid at short times and does not take into account the possibility of multiparticle couplings.

We conclude this section with hydrodynamic evaluations of the fifth-order signal. The density correlation function $F(\mathbf{k},t)$ can be evaluated via numerical simulations or with viscoelastic models.[60–63] The detailed description of the evaluation of $F(\mathbf{k},t)$ is introduced in Appendix E. Then, with $\bar{\mathbf{T}}_g(k)=T_g(k)\mathbf{D}$ and $T_g(k)=-\int d^3r g(r)j_2(kr)/r^3$ given in Ref. 20, we are able to evaluate Eq. (3.5) numerically. Figures 5 and 6 are the fifth-order response plotted along the diagonal cross section and the second time axis. In comparison with the fifth-order response function simulated by Ma and Stratt in Ref. 53, our prediction has roughly the same profile, but the peak position moves inward. Figure 7 is a two-dimensional contour of the predicted fifth-order signal and exhibits similar features as the numerical result. Therefore, the simple Gaussian factorization scheme provides a

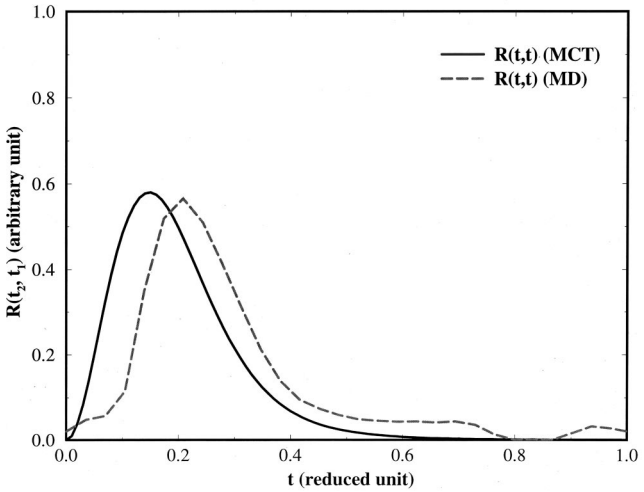

FIG. 5. Fifth-order response functions $R(t,t)$ from the hydrodynamic expression in Eq. (3.5) and from the MD simulation.

reliable way to predict the fifth-order Raman response in atomic liquids.

IV. TRANSFORMATION OF THE FIFTH-ORDER RESPONSE FUNCTION

A. Integrated intensity

As pointed out in Sec. I, we can reduce the two-dimensional response function to one-dimension correlation functions, which are easily examined for their angular and temporal dependencies. Integrating Eq. (1.1) along the first time variable, we obtain

$$\int_0^\infty R(t_2,t_1)dt_1 = -\beta\langle\{\mathbf{\Pi}(t_2),\mathbf{\Pi}(0)\}\mathbf{\Pi}(0)\rangle = \beta^2\langle\mathbf{\Pi}(t_2)\dot{\mathbf{\Pi}}(0)\mathbf{\Pi}(0)\rangle, \tag{4.1}$$

where the Poisson bracket $\{\mathbf{\Pi},\mathbf{\Pi}\}$ evaluated at the same time vanishes. However, the two pairs of polarization indices at time zero in the last expression of Eq. (4.1) are generally not the same, so the time derivative at time zero is not complete and the integrated response function cannot be directly transformed into a time-correlation function. To this end, we symmetrize these two pairs of polarization indices in Eq. (4.1),

$$R(t_2,t_1)_{s,\mu_2\nu_2\mu_1\nu_1\mu_0\nu_0} = \tfrac{1}{2}[R(t_2,t_1)_{\mu_2\nu_2\mu_1\nu_1\mu_0\nu_0} + R(t_2,t_1)_{\mu_2\nu_2\mu_0\nu_0\mu_1\nu_1}] \tag{4.2}$$

and obtain the desired relation

$$S_s(t_2) = \int_0^\infty R_s(t_2,t_1)dt_1 = -\beta^2\langle\dot{\mathbf{\Pi}}(t_2)\mathbf{\Pi}(0)\mathbf{\Pi}(0)\rangle_s = -\beta^2\frac{\partial}{\partial t_2}C_s(t_2), \tag{4.3}$$

where the symmetric correlation function $C_s(t) = \langle\mathbf{\Pi}(t)\mathbf{\Pi}(0)\mathbf{\Pi}(0)\rangle_s$ is defined similarly as in Eq. (4.2) and is the quantity for further calculations.

Within the renormalized DID approximation, the total polarizability tensor is written as the sum of the traceless part $\mathbf{\Pi}_D$ and the isotropic part $\mathbf{\Pi}_I$, i.e., $\mathbf{\Pi}=\mathbf{\Pi}_D+\mathbf{\Pi}_I$. Then, the symmetric correlation function $C_s(t)$ becomes

$$C_s(t) = \overline{\alpha}^6\langle\mathbf{\Pi}(t)\mathbf{\Pi}(0)\mathbf{\Pi}(0)\rangle_s = c_{s,DDD}C_{DDD}(t) + c_{s,IDD}C_{IDD}(t) + c_{s,DID}C_{DID}(t) + c_{s,DDI}C_{DDI}(t) + c_{s,III}C_{III}(t), \tag{4.4}$$

where the time-dependent parts depend on the details of interactions and the state of liquid. The coefficients depend on the polarization geometry and are symmetric with respect to the exchange of the second and last pairs of indices. Because of this symmetry, we have $c_{s,DDI}=c_{s,DID}=(c_{DDI}$

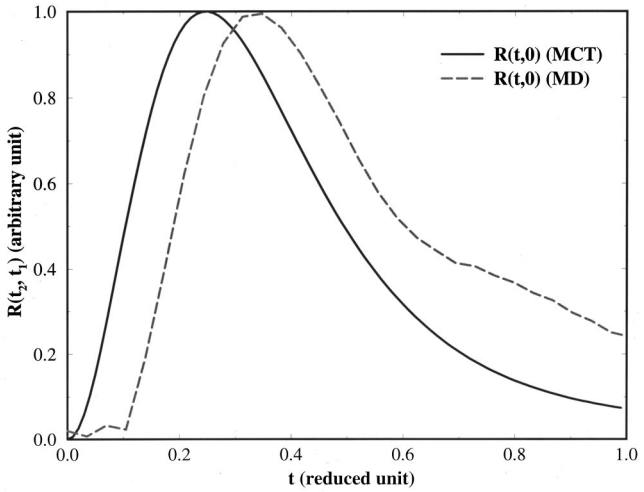

FIG. 6. Fifth-order response functions $R(t,0)$ from the hydrodynamic expression in Eq. (3.5) and from the MD simulation.

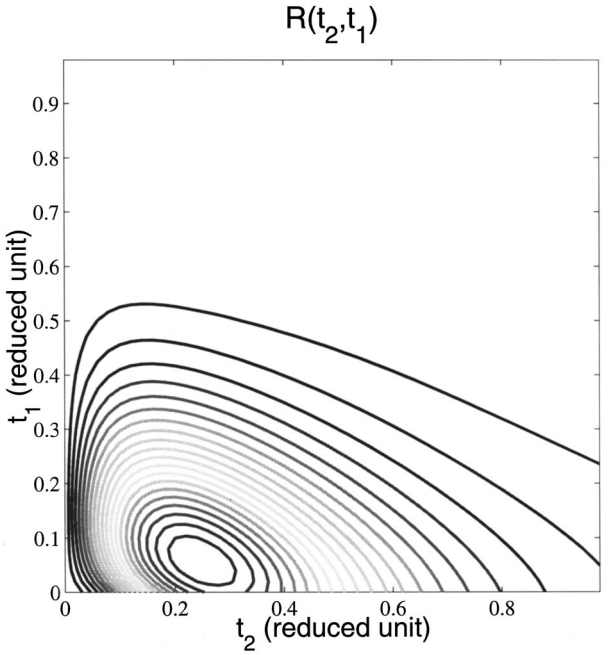

FIG. 7. Contour plot of the fifth-order response function $R(t_2,t_1)$ predicted by the molecular hydrodynamic expression Eq. (3.5).

TABLE III. Decomposition of the symmetric correlation function $C_s(t)$. The coefficients are normalized by the $ZZZZZZ$ component. The overlines stand for interchange of pairs of Raman indices.

	$C_s(t_2,t_1)$	$c_{s,DDD}$	$c_{s,IDD}\backslash c_{s,DDI}$	$c_{s,DID}$	$c_{s,III}$
C_1	$ZZZZZZ$	1	1	1	1
$C_2\backslash C_4$	$\overbrace{\overline{YY}ZZ\overline{ZZ}}$	$-1/2$	1/8	$-1/2$	1
C_3	$ZZYYZZ$	$-1/2$	$-1/2$	1	1
C_5	$ZZYYXX$	1	$-1/2$	$-1/2$	1
$C_6\backslash C_8$	$\overbrace{\overline{ZZ}ZY\overline{ZY}}$	$3/8+\delta c$	1/8	0	0
C_7	$ZYZZZY$	$3/8-2\delta c$	0	1/4	0
$C_9\backslash C_{11}$	$\overbrace{\overline{ZZ}XY\overline{XY}}$	$-3/4-2\delta c$	1/8	0	0
C_{10}	$XYZZXY$	$-3/4+4\delta c$	0	1/4	0
C_{12}	$ZYYXXZ$	9/16	0	0	0

$+c_{DID})/2$. Table III lists these coefficients normalized by the R_{zzzzzz} tensor component. Thus, the nine distinct tensor elements of the integrated intensity along the t_2 axis can be decomposed into four components within the renormalized Drude oscillator model. With a single time variable, the integrated response function provides more polarization selectivity than the third-order response function and thus is more useful for resolving microscopic interactions.

The integrated intensity for the fifth-order Raman response and the third-order Raman correlation function are both single time correlation functions but with different numbers (or weights) of total polarizability tensors. However, the two types of correlation functions share similar asymptotic behaviors, which are dictated by the interparticle diffusive motion. For example, as a rough estimation, we have

$$C_{DID}(t):C_{III}(t)\propto C_{\text{anoiso}}(t):C_{\text{iso}}(t), \tag{4.5}$$

which relates the fifth-order measurement to the third-order measurement.

B. Cumulative response function

As an alternative to the integrated response function, we now reduce the fifth-order Raman response to the cumulative response function. To do this, we integrate both sides of Eq. (1.1) along the t_1 axis and obtain

$$\begin{aligned} S(t_2,t_1)&=\int_{t_1}^{\infty}R(t_2,\tau)d\tau=-\beta B(t_1,t_2),\\ S'(t_2,t_1)&=\int_{0}^{t_1}R(t_2,\tau)d\tau=\beta[B(t_2,t_1)-B(t_2,0)], \end{aligned} \tag{4.6}$$

where the two-dimensional function $S(t_2,t_1)$ and $S'(t_2,t_1)$ are the cumulative response function integrated along the t_1 axis. The function $B(t_2,t_1)$ is expressed as

$$\begin{aligned} B(t_2,t_1)&=\langle\{\mathbf{\Pi}_2(t_2+t_1),\mathbf{\Pi}_1(t_1)\}\mathbf{\Pi}_0(0)\rangle\\ &=-\beta\langle\mathbf{\Pi}_2(t_2+t_1)\dot{\mathbf{\Pi}}_1(t_1)\mathbf{\Pi}_0(0)\rangle+\langle\mathbf{\Pi}_2(t_2+t_1)\\ &\quad\times\{\mathbf{\Pi}_1(t_1)\mathbf{\Pi}_0(0)\}\rangle. \end{aligned} \tag{4.7}$$

The last term in Eq. (4.7) can be rearranged as

$$\begin{aligned} &\langle\mathbf{\Pi}_2(t_2+t_1)\{\mathbf{\Pi}_1(t_1)\mathbf{\Pi}_0(0)\}\rangle\\ &\quad=-\langle\{\mathbf{\Pi}_0(0),\mathbf{\Pi}_1(t_1)\}\mathbf{\Pi}_2(t_2+t_1)\rangle\\ &\quad=\langle\{\mathbf{\Pi}_0(t_2+t_1),\mathbf{\Pi}_1(t_2)\}\mathbf{\Pi}_2(0)\rangle, \end{aligned} \tag{4.8}$$

where the time-reversal symmetry is invoked in the last step. However, the two tensor elements $\mathbf{\Pi}_0$ and $\mathbf{\Pi}_2$ in Eq. (4.8) expression are generally not the same. To symmetrize these two tensor elements, we define

$$\begin{aligned} R(t_2,t_1)_{s,\mu_2\nu_2\mu_1\nu_1\mu_0\nu_0}&=\tfrac{1}{2}[R(t_2,t_1)_{\mu_2\nu_2\mu_1\nu_1\mu_0\nu_0}\\ &\quad+R(t_2,t_1)_{\mu_0\nu_0\mu_1\nu_1\mu_2\nu_2}] \end{aligned} \tag{4.9}$$

and similarly for F_s and C_s, so that Eq. (4.7) leads to the desired relation

$$F_s(t_2,t_1)-F_s(t_1,t_2)=-\beta\dot{C}_s(t_2,t_1), \tag{4.10}$$

where $\dot{C}_s(t_2,t_1)=\langle\mathbf{\Pi}_2\dot{\mathbf{\Pi}}_1\mathbf{\Pi}_0\rangle=(\partial_1-\partial_2)C_s(t_2,t_1)$. Substituting the above relation in Eq. (4.10) for F_s back into Eq. (4.7), we have

$$\begin{aligned} S_s(t_2,t_1)-S_s(t_1,t_2)&=\beta^2\dot{C}_s(t_2,t_1),\\ S_s'(t_2,t_1)-S_s'(t_1,t_2)&=\beta^2\dot{C}_s(t_2,t_1)+\beta^2\dot{C}_s(t_2,0)\\ &\quad-\beta^2\dot{C}_s(0,t_1), \end{aligned} \tag{4.11}$$

which relate the cumulative response function to two-time correlation functions.

The two-time symmetric correlation function is a special case of the two-time correlation function discussed in Sec. II and can be decomposed using the same symmetry considerations as in Sec. II C, giving

$$\begin{aligned} C_s(t_2,t_1)&=c_{s,DDD}C_{DDD}(t_2,t_1)+c_{s,IDD}C_{IDD}(t_2,t_1)\\ &\quad+c_{s,DID}C_{DID}(t_2,t_1)+c_{s,DDI}C_{DDI}(t_2,t_1)\\ &\quad+c_{s,III}C_{III}(t_2,t_1), \end{aligned} \tag{4.12}$$

where the time-dependent parts are the same as in Eq. (2.19). The coefficients are symmetric with respect to the exchange of the first and last pairs of indices. Out of the five symmetric coefficients, three are identical to the original definition in Eq. (2.19), i.e., $c_{s,DDD}=c_{DDD}$, $c_{s,DID}=c_{DID}$, and $c_{s,III}=c_{III}$, whereas the other two are equal, i.e., $c_{s,DDI}=c_{s,IDD}=(c_{DDI}+c_{IDD})/2$. These symmetric coefficients are listed in Table IV with the normalization condition defined by the R_{zzzzzz} tensor element.

C. Symmetric correlation function

As shown in Sec. IV B, the symmetric cumulative response function $S_s(t_2,t_1)$ is related to the symmetric two-time correlation function by

$$S_s(t_2,t_1)-S_s(t_1,t_2)=\beta^2\dot{C}_s(t_2,t_1), \tag{4.13}$$

TABLE IV. Decomposition of the symmetric correlation function $C_s(t_2,t_1)$. The coefficients are normalized by the $ZZZZZZ$ component. The overbars stand for the interchange of pairs of Raman indices.

	$C_s(t)$	c_{DDD}	c_{IDD}	$c_{DID}\backslash c_{DDI}$	c_{III}
C_1	$ZZZZZZ$	1	1	1	1
C_2	$YYZZZZ$	$-1/2$	1	$-1/2$	1
$C_3\backslash C_4$	$ZZ\overbrace{YY\,ZZ}$	$-1/2$	$-1/2$	1/4	1
C_5	$ZZYYXX$	1	$-1/2$	$-1/2$	1
C_6	$ZZZYZY$	$3/8-\delta c$	1/4	0	0
$C_7\backslash C_8$	$ZY\overbrace{ZZ\,ZY}$	$3/8+\delta c/2$	0	1/8	0
C_9	$ZZXYXY$	$-3/4-2\,\delta c$	1/4	0	0
$C_{10}\backslash C_{11}$	$XY\overbrace{ZZ\,XY}$	$-3/4+\delta c$	0	1/8	0
C_{12}	$ZYYXXZ$	9/16	0	0	0

where $\dot{C}_s(t_2,t_1)=(\partial_1-\partial_2)C_s(t_2,t_1)$. Here, the correlation function and related quantities are completely symmetric with respect to the exchange of pairs of the indices,

$$C_{s,\mu_2\nu_2\mu_1\nu_1\mu_0\nu_0}=\tfrac{1}{6}[C_{\mu_2\nu_2\mu_1\nu_1\mu_0\nu_0}+C_{\mu_2\nu_2\mu_0\nu_0\mu_1\nu_1}+C_{\mu_1\nu_1\mu_2\nu_2\mu_0\nu_0}+C_{\mu_1\nu_1\mu_0\nu_0\mu_2\nu_2}+C_{\mu_0\nu_0\mu_1\nu_1\mu_2\nu_2}+C_{\mu_0\nu_0\mu_2\nu_2\mu_1\nu_1}]. \quad (4.14)$$

The two time variables t_1 and t_2 are transformed into a new set of variables $\tau_1=(t_1+t_2)/2$ and $\tau_2=(t_2-t_1)/2$ so that Eq. (4.14) in the new coordinates becomes

$$S_s(\tau_1+\tau_2,\tau_1-\tau_2)-S_s(\tau_1-\tau_2,\tau_1+\tau_2)=-\beta^2\frac{\partial}{\partial\tau_2}C_s(\tau_1+\tau_2,\tau_1-\tau_2). \quad (4.15)$$

Explicit integration of Eq. (4.15) over τ_2 from $(t_2-t_1)/2$ to $(t_2+t_1)/2$ along the coordinate axis $\tau_1=(t_2+t_1)/2$ gives

$$\beta^2[C_s(t_2,t_1)-C_s(t_2+t_1,0)]=\int_{(t_2-t_1)/2}^{(t_2+t_1)/2}[S_s(\tau_1+\tau_2,\tau_1-\tau_2)-S_s(\tau_1-\tau_2,\tau_1+\tau_2)]d\tau_2. \quad (4.16)$$

Since $C_s(t_2+t_1,0)$ is symmetric under the exchange of $\mu_1\nu_1$ and $\mu_0\nu_0$, $C_s(t_2+t_1,0)$ can be obtained by integrating Eq. (4.3) along the t_2 axis, giving

$$\beta^2C_s(t_2+t_1,0)=\int_{t_2+t_1}^{\infty}S_s(\tau,0)d\tau. \quad (4.17)$$

Thus, the overall relation between the symmetric two-time correlation function and the cumulative response function $S_s(t_2,t_1)$ becomes

$$\beta^2C_s(t_2,t_1)=\int_{t_1+t_2}^{\infty}S_s(\tau,0)d\tau+\int_{(t_2-t_1)/2}^{(t_2+t_1)/2}\left[S_s\left(\frac{t_2+t_1}{2}+\tau_2,\frac{t_2+t_1}{2}-\tau_2\right)-S_s\left(\frac{t_2+t_1}{2}-\tau_2,\frac{t_2+t_1}{2}+\tau_2\right)\right]d\tau_2. \quad (4.18)$$

In principle, given the complete information of the response function $R(t_2,t_1)$ on the (t_2,t_1) plane, the completely symmetric two-time correlation function can be obtained from Eq. (4.8).

As shown in Appendix A, the fifth-order Raman response function cannot be directly written as a correlation function without involving the stability matrix, which contains information about the coherence of motion. This information is lost as the fifth-order Raman response function, $R_s(t_2,t_1)$, which is not symmetric with respect to t_1 and t_2 variables, is transformed into $C_s(t_2,t_1)$, which is symmetric with respect to t_1 and t_2 variables. However, the resulting correlation function from the transformation has the advantage of the reliable predictions for their time dependence and polarization dependence, thus providing both a self-consistent check of numerical simulations and an easy comparison with experimental measurements.

D. Numerical results

As a numerical example, we compare the three kinds of time-correlation functions obtained directly from our molecular dynamics simulations with the corresponding results generated from the fifth-order Raman response function provided by Ma and Stratt.[53] To be consistent with their published result, our simulation was carried out with 108 Xe atoms at reduced density and reduced temperature T^*

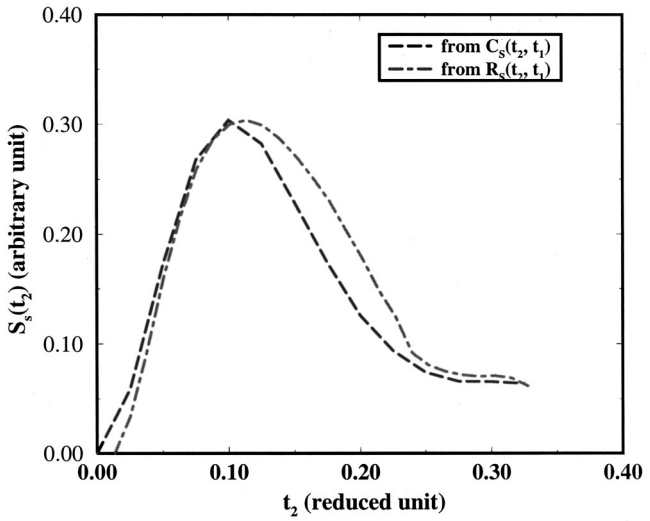

FIG. 8. A plot of the integrated intensity $S_{zzzzzz}(t_2)$ of liquid Xe. The dashed line is directly obtained from our MD simulation, and the dotted line is generated from the fifth-order response function data calculated by Ma and Stratt. The molecular dynamics simulation was carried out for a simulation box of 108 Xe atoms at reduced temperature $T^*=1.0$ and reduced density $\rho^*=0.80$.

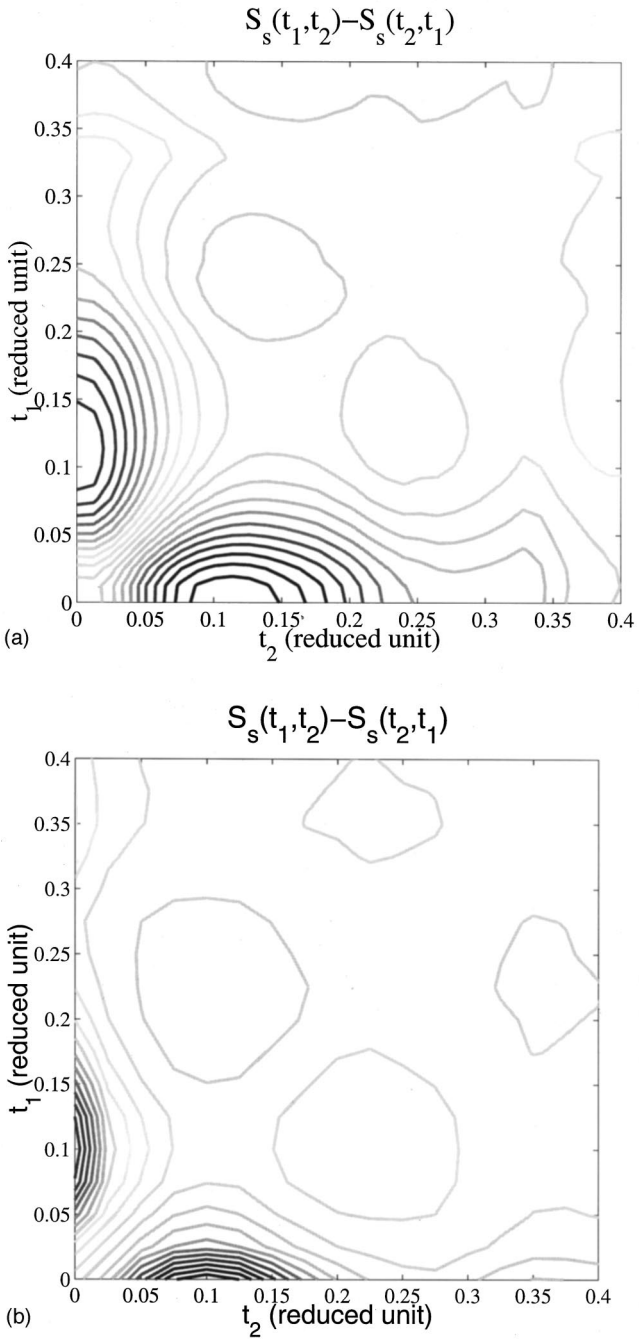

FIG. 9. A comparison of the cumulative response functions $S_s(t_1,t_2)-S_s(t_2,t_1)$ (a) generated from the fifth-order response function data and (b) obtained directly from the MD simulation.

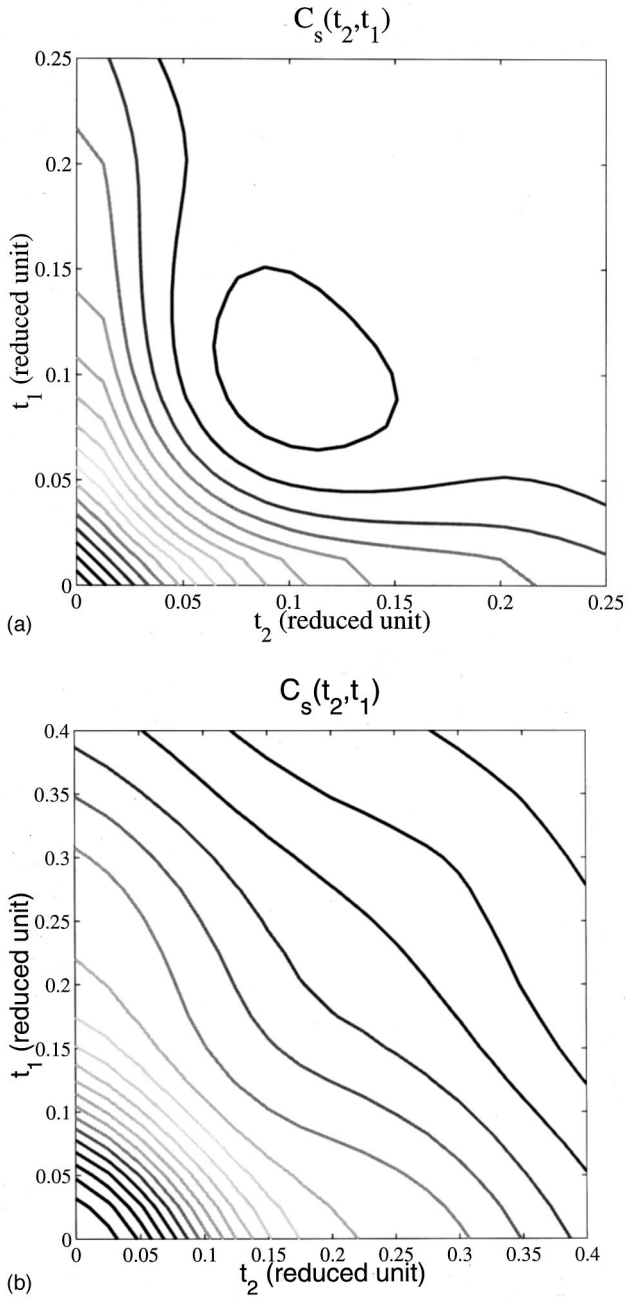

FIG. 10. A comparison of the symmetrized two-time correlation functions $C_s(t_2,t_1)$ (a) generated from the fifth-order response function data and (b) obtained directly from the MD simulation.

$=1.00$ and $\rho^*=0.8$, and all the results are presented for the *zzzzzz* polarization component. Details of numerical simulations can be found in Paper I.

Figure 8 plots the integrated intensity $S_s(t_2)$ in Sec. IV A from our direct numerical simulation and from the integration of the two-dimensional spectrum by Ma and Stratt. Both curves have a broad peak centered at around $t^*=0.1$. The peak position corresponds to the t_2 projection of the elongated maximal of two-dimensional response function. The integrated intensity has a slightly different shape from the third-order correlation function calculated in Paper I, because of the weights of the total polarizability are different.

Figure 9(a) is the cumulative response function $S_s(t_1,t_2)-S_s(t_2,t_1)$ generated from the data of the fifth-order Raman response function. For comparison, Fig. 9(b) is the function $-\beta^2\dot{C}_s(t_2,t_1)$ obtained directly from our numerical simulation, as discussed in Sec. IV B. Both contours show a clear maximum around $t_2^*=0.1$ along t_2 axis and a corresponding minimum along t_1 due to the fact that $S_s(t_1,t_2)-S_s(t_2,t_1)$ is an antisymmetric function. The shapes of the contours in Figs. 9(a) and 9(b) are similar though the details differ because of the different approaches.

As described in Sec. IV C, the symmetrized two-time correlation function $C_s(t_2,t_1)$ can be integrated from the fifth-order response function. The result thus obtained is

TABLE V. Decomposition of the completely symmetric correlation function $C_s(t_2,t_1)$. The coefficients are normalized by the $ZZZZZZ$ component. The overbars stand for the interchange of pairs of Raman indices.

	$C_s(t_2,t_1)$	$c_{s,DDD}$	$c_{s,IDD}\backslash c_{s,DDI}\backslash c_{s,DID}$	$c_{s,III}$
C_1	$\overline{ZZZZZZ}$	16/35	4/5	1
$C_2\backslash C_3\backslash C_4$	$\overline{YYZZZZ}$	−8/35	0	1
C_5	$\overline{ZZYYXX}$	16/35	−2/5	1
$C_6\backslash C_7\backslash C_8$	$\overline{ZZZYZY}$	6/35	1/15	0
$C_9\backslash C_{10}\backslash C_{11}$	$\overline{ZZXYXY}$	−12/35	1/15	0
C_{12}	$\overline{ZYYXXZ}$	9/35	0	0

plotted in Fig. 10(a) along with the MD simulation result in Fig. 10(b). Evidently, the two contours share similar structures, and the difference at large times is mainly due to the truncation in the time integration of the response function.

V. CONCLUSIONS

In summary, the symmetry of the polarizability tensor $\mathbf{\Pi}$ completely characterizes the decomposition into independent polarization components, and is independent of the type of liquids, the form of interaction potentials, or the description of particle motions. For an isotropic medium, the fifth-order Raman correlation function and response function have twelve distinct tensor elements. These elements are subject to the constraints imposed by the rotational symmetry and time reversal symmetry, and hence can be decomposed into seven independent components for the correlation function and ten independent components for the response function. The decomposition coefficients are calculated and tabulated explicitly and can be used to describe interactions and couplings in atomic liquids (Table V).

The temporal profile of the fifth-order signal in atomic liquids is calculated using the Gaussian factorization scheme. The derivation is simple and the result is useful as it relates the fifth-order response function to density fluctuations. As an alternative, the fifth-order response function can be reduced to two-time and single-time correlation functions, which are relatively simple to compute and analyze. Particularly, the integrated intensity in Sec. IV A is a single-time correlation function and can be related to the third-order Raman response.

We have investigated the angular dependence and temporal profile of the fifth-order Raman signal in liquid Xe. A basic assumption of the study is the use of the renormalized Drude oscillator model, which takes into account the many-body polarization effects and particularly its contribution to the isotropic polarization component. Future studies will be directed toward modeling nonlinear spectra in molecular liquids.

ACKNOWLEDGMENTS

The research is supported by the AT&T Research Fund Award, the Petroleum Research Fund administrated by the American Chemical Society, and the NSF Career Award (No. Che-0093210). We thank R.A. Denny, D.R. Reichman and A. Tokmakoff for discussions and comments. We thank Ma and Stratt for providing their simulation data of C_{zzzzzz} of liquid Xe.

APPENDIX A: THREE EXPLICIT EXPRESSIONS OF THE FIFTH-ORDER RAMAN RESPONSE FUNCTION

The fifth-order Raman response function is defined in terms of the Poisson bracket in Eq. (1.1). Explicit evaluation of the Poisson brackets leads to several equivalent expressions, which can be useful for different purposes. For simplicity, the total polarizability operator is taken as a function of the coordinate only and is independent of the momentum.

As the simplest expression, we have

$$R(t_2,t_1)=-\beta\langle\{\mathbf{\Pi}_2,\mathbf{\Pi}_1\}\dot{\mathbf{\Pi}}_0\rangle=\beta\left\langle\frac{\partial\mathbf{\Pi}_2}{\partial r_{2i}}\frac{\partial r_{2i}}{\partial p_{1j}}\frac{\partial\mathbf{\Pi}_1}{\partial r_{1j}}\dot{\mathbf{\Pi}}_0\right\rangle, \tag{A1}$$

where the subscripts 1 and 2 refer to time t_1+t_2 and t_1, respectively, the subscripts i and j refer to the atomic degrees of freedom, repeated indices are summed over explicitly, and $\partial r_{2i}/\partial p_{1j}=M_{ij}(t_1,t_2)$ is the stability matrix element.

The second expression follows Mukamel's derivation,

$$\begin{aligned}R(t_2,t_1)&=-\beta\langle\{\mathbf{\Pi}_2,\mathbf{\Pi}_1\}\dot{\mathbf{\Pi}}_0\rangle\\&=\beta^2\langle\mathbf{\Pi}_2\dot{\mathbf{\Pi}}_1\dot{\mathbf{\Pi}}_0\rangle-\beta\langle\mathbf{\Pi}_2\{\mathbf{\Pi}_1,\dot{\mathbf{\Pi}}_0\}\rangle\\&=\beta^2\langle\mathbf{\Pi}_2\dot{\mathbf{\Pi}}_1\dot{\mathbf{\Pi}}_0\rangle\\&\quad-\beta\left\langle\mathbf{\Pi}_2\frac{\partial\mathbf{\Pi}_1}{\partial r_{1j}}\left(\frac{\partial r_{1j}}{\partial r_{0i}}\frac{\partial\dot{\mathbf{\Pi}}_0}{\partial p_{0i}}-\frac{\partial r_{1j}}{\partial p_{0i}}\frac{\partial\dot{\mathbf{\Pi}}_0}{\partial r_{0i}}\right)\right\rangle,\end{aligned} \tag{A2}$$

where the first term has the form of the correlation function but the second term involves the stability matrix.

To obtain the third expression, we start from the inner Poisson bracket and explicitly expand the outer Poisson bracket

$$\begin{aligned}R(t_2,t_1)&=-\left\langle\left\{\frac{\partial\mathbf{\Pi}_2}{\partial r_{2j}}\frac{\partial r_{2j}}{\partial p_{1i}}\frac{\partial\mathbf{\Pi}_1}{\partial r_{1i}},\mathbf{\Pi}_0\right\}\right\rangle\\&=\left\langle\frac{\partial}{\partial p_{0k}}\left[\frac{\partial\mathbf{\Pi}_2}{\partial r_{2j}}\frac{\partial r_{2j}}{\partial p_{1i}}\frac{\partial\mathbf{\Pi}_1}{\partial r_{1i}}\right]\frac{\partial\mathbf{\Pi}_0}{\partial r_{0k}}\right\rangle\\&=\left\langle\left[\frac{\partial^2\mathbf{\Pi}_2}{\partial r_{2j}\partial r_{2l}}\frac{\partial\mathbf{\Pi}_1}{\partial r_{1i}}\frac{\partial r_{2l}}{\partial p_{0k}}\frac{\partial r_{2j}}{\partial p_{1i}}\right.\right.\\&\quad+\frac{\partial\mathbf{\Pi}_2}{\partial r_{2j}}\frac{\partial^2\mathbf{\Pi}_1}{\partial r_{1i}\partial r_{1l}}\frac{\partial r_{1l}}{\partial p_{0k}}\frac{\partial r_{2j}}{\partial p_{1i}}\\&\quad\left.\left.+\frac{\partial\mathbf{\Pi}_2}{\partial r_{2j}}\frac{\partial\mathbf{\Pi}_1}{\partial r_{1i}}\frac{\partial^2 r_{2j}}{\partial p_{1i}\partial p_{0k}}\right]\frac{\partial\mathbf{\Pi}_0}{\partial r_{0k}}\right\rangle.\end{aligned} \tag{A3}$$

As an approximation, we omit the last term, treat the derivatives of the polarizability as a static weight, $\rho(\omega)=\langle\delta(\omega-\omega(\mathbf{r}))\partial^2\mathbf{\Pi}/\partial\mathbf{r}^2(\partial\mathbf{\Pi}/\partial\mathbf{r})^2\rangle$, and assume that the dynamics is governed by harmonic oscillator motions with frequency ω. Consequently,

$$R(t_2,t_1)=\int d\omega\,\rho(\omega)\frac{1}{(m\omega)^2}\sin(\omega t_2)\times[\sin(\omega t_1+\omega t_2)+\sin(\omega(t_1)], \tag{A4}$$

which is the instantaneous normal mode expression for the fifth-order Raman response function. It is not difficult to introduce two different frequencies ω_1 and ω_2 for the two time intervals. The recent simulation by Ma and Stratt [53] indicates that the joint distribution of the two frequencies, $\rho(\omega_1,\omega_2)$, is dominated by the diagonal cross-section $\omega_1=\omega_2$. So it is reasonable to use a single frequency in the instantaneous normal mode analysis.

APPENDIX B: DRUDE OSCILLATOR MODEL

The Drude oscillator model consists of oscillating dipoles with polarizability α interacting through the second-order dipole tensor $\mathbf{T}$. The total polarizability tensor of a fluid composed of N identical spherical Drude oscillators is

$$\mathbf{\Pi}(t)=\sum_{i\neq j}^{N}\alpha[\mathbf{I}-\alpha\mathbf{T}(t)]^{-1}_{ij}, \tag{B1}$$

where the summation is carried over all pair of particles, and $\mathbf{\Pi}$ is a function of evolving liquid configuration through the time dependence in $\mathbf{T}_{ij}(t)=\mathbf{T}[\mathbf{r}_{ij}(t)]$. The dipole–dipole interaction tensor is defined as $T_{\mu\nu}(\mathbf{r})=D_{\mu\nu}(\hat{\mathbf{r}})/r^3$, where μ and ν denote the three Cartesian coordinates, $\mathbf{r}$ is the vector connecting a pair of liquid particles, $\hat{\mathbf{r}}=\mathbf{r}/r$ is the corresponding unit vector, and $\mathbf{D}$ is the traceless dimensionless tensor $\mathbf{D}(\hat{\mathbf{r}})=3\hat{\mathbf{r}}\hat{\mathbf{r}}-\mathbf{I}$. The many-body polarization effect in Eq. (B1) leads to an infinite expression in terms of $\mathbf{T}$, which to the leading other truncation of $\mathbf{\Pi}$ results in the pair interaction approximation

$$\mathbf{\Pi}\approx\sum_{i}\alpha+\sum_{i\neq j}\alpha\mathbf{T}_{ij}\alpha, \tag{B2}$$

where the first term is a constant and the second term corresponds to the first-order dipole–induced-dipole interaction (DID). Because T is a traceless tensor, the pair interaction in Eq. (B2) represents the anisotropic part of the DID polarizability. To account for the isotropic DID polarizability, it is necessary to include the next term, $\alpha^3\mathbf{T}_{ik}\mathbf{T}_{kj}$, in the expansion of Eq. (B2). We explicitly evaluated the three-body term in Paper I and found that the anisotropic part of the DID interaction is long-ranged whereas the isotropic part of the DID interaction is short-ranged. The approximate resummation of the infinite terms in the expansion leads to a renormalized DID form for the total polarizability,

$$\mathbf{\Pi}\approx\sum_{i}\bar{\alpha}+\sum_{i\neq j}\bar{\alpha}\bar{\mathbf{T}}_{ij}\bar{\alpha}=\sum_{i}\bar{\alpha}+\sum_{i\neq j}\bar{\alpha}(h_I\mathbf{I}+h_D\mathbf{D})\bar{\alpha}, \tag{B3}$$

where h_D is the traceless anisotropic part and h_I is the diagonal isotropic part. The renormalized quantities $\bar{\alpha}$ and $\mathbf{T}$ are solved self-consistently in Paper I.

APPENDIX C: ROTATIONAL SYMMETRY OF THE TWO-TIME CORRELATION FUNCTION

As shown in Sec. II, a large number of tensor elements are identical so that only twelve distinct elements are calculated. These twelve elements are used to define three sets of totally symmetric correlation functions in Eqs. (2.2)–(2.4) which are related to each other through rotation invariance. Explicitly, rotational symmetry of an isotropic sample preserves the value of a tensor element under the rotation about any angle,

$$C_{\mu_2\nu_2\mu_1\nu_1\mu_0\nu_0}=R_{\mu_2\mu_2'}R_{\nu_2\nu_2'}R_{\mu_1\mu_1'}R_{\nu_1\nu_1'}R_{\mu_0\mu_0'}R_{\nu_0\nu_0'}C_{\mu_2'\nu_2'\mu_1'\nu_1'\mu_0'\nu_0'} \tag{C1}$$

where R is the rotational transformation matrix. For example, we consider the rotation around the X axis through an angle in the ZY plane. The application of Eq. (C1) to the C_{zzzzzz} gives

$$Z_z=\cos^6(\theta)Z_z+\cos^4(\theta)\sin^2(\theta)Z_{zy}+\cos^2(\theta)\sin^4(\theta)Z_{yz}+\sin^6(\theta)Z_y, \tag{C2}$$

which simplifies to $3Z_\mu=Z_{\mu\nu}$. For $Z_{\mu\nu}$ components, we have

$$Z_{zx}=\cos^4(\theta)Z_{zx}+\sin^4(\theta)Z_{yx}+6\sin^2(\theta)\cos^2(\theta)Z_{zyx}, \tag{C3}$$

which results in $3Z_{\mu\nu\gamma}=Z_{\mu\nu}$. These relations have been obtained by Tokmakoff and are included here for completeness.[34]

APPENDIX D: DERIVATION OF THE HYDRODYNAMIC EXPRESSION USING QUANTUM OPERATORS

We now repeat the hydrodynamic evaluation of the fifty-order Raman response by taking the classical limit of quantum operators after the Gaussian factorization. The response function in Eq. (1.1) is defined quantum mechanically as

$$\begin{aligned}R(t_2,t_1)&=-\frac{1}{\hbar^2}\langle[\hat{\mathbf{\Pi}}(t_2+t_1),\hat{\mathbf{\Pi}}(t_1)],\hat{\mathbf{\Pi}}(0)]\rangle\\&=-\frac{1}{\hbar^2}\langle\hat{\mathbf{\Pi}}_2\hat{\mathbf{\Pi}}_1\hat{\mathbf{\Pi}}_0-\hat{\mathbf{\Pi}}_1\hat{\mathbf{\Pi}}_2\hat{\mathbf{\Pi}}_0-\hat{\mathbf{\Pi}}_0\mathbf{\Pi}_2\hat{\mathbf{\Pi}}_1\\&\quad+\hat{\mathbf{\Pi}}_0\hat{\mathbf{\Pi}}_1\hat{\mathbf{\Pi}}_2\rangle,\end{aligned} \tag{D1}$$

where $\mathbf{\Pi}$ is the Heisenberg operator for the total polarizability. With the Fourier expression of $\mathbf{\Pi}$ given in Eq. (4.1), the first term in Eq. (D1) can be evaluated explicitly, giving

$$\begin{aligned}&\langle\hat{\mathbf{\Pi}}(t_2+t_1)\hat{\mathbf{\Pi}}(t_1)\hat{\mathbf{\Pi}}(0)\rangle\\&=\left(\frac{\bar{\alpha}^2}{V}\right)^3\sum\bar{\mathbf{T}}(\mathbf{k}_2)\bar{\mathbf{T}}(\mathbf{k}_1)\bar{\mathbf{T}}(\mathbf{k})\langle\hat{\rho}_2\hat{\rho}_2^+\hat{\rho}_1\hat{\rho}_1^+\hat{\rho}_0\hat{\rho}_0^+\rangle\\&\approx 4\left(\frac{N\bar{\alpha}^2}{V}\right)^3\sum\bar{\mathbf{T}}(\mathbf{k})\bar{\mathbf{T}}(\mathbf{k})\bar{\mathbf{T}}(\mathbf{k})\hat{F}(t_1+t_2,\mathbf{k})\\&\quad\times\hat{F}(t_2,-\mathbf{k})\hat{F}(t_1,-\mathbf{k}),\end{aligned} \tag{D2}$$

where the density operators at different times do not commute. The approximation arises from the application of the

Gaussian factorization scheme, and the factor of 4 arises from the different ways of decomposition. Combining the four terms in Eq. (D1), we obtain

$$\begin{aligned}&\hat{F}(t_1+t_2,\mathbf{k})\hat{F}(t_2,-\mathbf{k})\hat{F}(t_1,-\mathbf{k})-\hat{F}(t_1+t_2,-\mathbf{k})\\&\times\hat{F}(-t_2,-\mathbf{k})\hat{F}(t_1,\mathbf{k})-\hat{F}(-t_1-t_2,-\mathbf{k})\\&\times\hat{F}(t_2,-\mathbf{k})\hat{F}(-t_1,-\mathbf{k})+\hat{F}(-t_1-t_2,\mathbf{k})\\&\times\hat{F}(-t_2,-\mathbf{k})\hat{F}(-t_1,-\mathbf{k})=[\hat{F}(t_2,-\mathbf{k})-\hat{F}(-t_2,\mathbf{k})]\\&\times[\hat{F}(t_1+t_2,\mathbf{k})\hat{F}(t_1,-\mathbf{k})-\hat{F}(-t_1-t_2,-\mathbf{k})\hat{F}(-t_1,\mathbf{k})\\&=(i\beta\hbar)^2\partial_2F(t_2,\mathbf{k})\partial_1[F(t_1+t_2,\mathbf{k})F(t_2,\mathbf{k})],\end{aligned}\tag{D3}$$

where we have rearranged the second and fourth terms in Eq. (D3) via $\mathbf{k}\rightarrow-\mathbf{k}$ and used the quantum-classical correspondence: $\hat{F}(t,\mathbf{k})-\hat{F}(-t,\mathbf{k})=i\hbar\beta\dot{F}(t)$. Taking the continuous limit of $\mathbf{k}$ and replacing the potential with the dressed potential, we arrive at the final expression

$$\begin{aligned}R(t_2,t_1)=&N\rho^2(\beta\hbar)^2\overline{\alpha^6}\frac{4}{(2\pi)^3}\\&\times\int d\mathbf{k}\,\overline{\mathbf{T}}_g(\mathbf{k})\overline{\mathbf{T}}_g(\mathbf{k})\overline{\mathbf{T}}_g(\mathbf{k})\partial_2F(t_2,\mathbf{k})\partial_1\\&\times[F(t_1+t_2,\mathbf{k})F(t_2,\mathbf{k})],\end{aligned}\tag{D4}$$

which is the same as Eq. (3.5) derived with the classical Poisson bracket and similar to the MCT result published by Denny and Reichman.[58]

APPENDIX E: HYDRODYNAMIC EVALUATION OF THE INTERMEDIATE SCATTERING FUNCTION

Here we summarize the molecular hydrodynamic expressions we used to evaluate the fifth-order signal, all the derivations can be found in Ref. 60. From the full hydrodynamic description, we obtain a set of coupled equations that take into account of the effects of temperature fluctuations,

$$\begin{aligned}&\frac{\partial}{\partial t}j_k^l(t)=ikc_T^2n_k(t)-\nu_lk^2j_k^l(t)+ikn\alpha c_T^2T_k(t),\\&nC_v\frac{\partial}{\partial t}T_k(t)=\frac{C_v}{\alpha}(\gamma-1)\frac{\partial}{\partial t}n_k(t)-\frac{\kappa k^2}{M}T_k(t),\\&\frac{\partial}{\partial t}n_k(t)=ikj_k^l(t),\end{aligned}\tag{E1}$$

where $j_k^l(t)$ is the longitudinal current, $n_k(t)$ is the local number density, $T_k(t)$ is the local temperature, α is the thermal expansion coefficient, $\gamma=C_p/C_v$ is the specific heat ratio, C_p and C_v are the specific heat at constant pressure and at constant volume, respectively, ν_l is the kinematic longitudinal viscosity coefficient, c_T is the isothermal sound velocity, and κ is the thermal conductivity coefficient. The generalized Langevin equation for the longitudinal current correlation function is

$$\frac{\partial}{\partial t}J_l(k,t)=-\int_0^t dt'\,K_l(k,t-t')J_l(k,t'),\tag{E2}$$

where $K_l(k,t)$ is the memory function for $J_l(k,t)$, given by

$$K_l(k,t)=\frac{(kv_0)^2}{S(k)}+k^2\Phi_l(k,t)+\frac{(kv_0)^2}{S(k)}(\gamma-1)e^{-D_Tk^2t},\tag{E3}$$

where $D_T=\kappa/(nMC_v)$, $S(k)$ is the static structure factor, and $\Phi_l(k,t)$ is the longitudinal viscosity function. When $\Phi_l(k,t)=2\nu_l\delta(t)$, $K_l(k,t)$ reduces to the linearized hydrodynamic approximation for the memory function obtained from Eq. (E1). The viscoelastic approximation leads to a generalized longitudinal viscosity function $\Phi_l(k,t)$ without modifying the thermal conductivity contribution

$$\begin{aligned}&\Phi_l(k,t)=\Phi_l(k,0)\exp[-t/\tau_l(k)],\\&\Phi_l(k,0)=\frac{\omega_l^2(k)}{(kv_0)^2}-\gamma\frac{v_0^2}{S(k)}.\end{aligned}\tag{E4}$$

The second frequency moment $\omega_l^2(k)$ can be calculated from the pair distribution function $g(r)$ and the pair potential $u(r)$ as follows:

$$\omega_l^2(k)=3k^2v_0^4+\frac{nv_0^2}{M}\int d^3\,rg(r)\frac{\partial^2u}{\partial z^2}(1-\cos kz).\tag{E5}$$

An empirical prescription for the relaxation time $\tau_l(k)$ is given by Akcasu and Daniels as[64]

$$\begin{aligned}\frac{1}{\tau_l^2(k)}=&\frac{8}{3}[c_\infty^2(k)-c_0^2(k)-v_0^2]k^2+\left(1+\frac{k^2}{k_l^2}\right)^{-1}\\&\times\left\{\frac{1}{\tau_l^2(0)}-\frac{8}{3}[c_\infty^2(0)-c_0^2(0)-v_0^2]k^2\right\},\end{aligned}\tag{E6}$$

where $k_l=1.5\,\text{Å}$, $c_\infty(k)$ and $c_0(k)$ are the high-frequency and the low-frequency sound velocities, respectively,

$$\begin{aligned}&c_0(k)=v_0\sqrt{\frac{\gamma}{S(k)}},\\&c_\infty(k)=\left\{\frac{1}{nM}\left[\frac{4}{3}G_\infty(k)+K_\infty(k)\right]\right\}^{1/2},\\&\frac{1}{\tau_l(0)}=\frac{c_\infty^2(0)-c_0^2(0)}{\frac{4}{3}\eta+\eta_B}.\end{aligned}\tag{E7}$$

This empirical form of $\tau_l(k)$ combines the elastic solid behavior at high frequency and the liquid behavior at low frequency, while still retaining the property of $\tau_l(0)$ as a Maxwell relaxation time. Substituting this form of $K_l(k,t)$ into the GLE for the longitudinal current correlation function $J_l(k,t)$, we obtain

$$J_l(k,\omega)=v_0^2\frac{\omega^2k^2D'(k,\omega)}{[\omega^2-(kv_0)^2/S(k)+\omega k^2D''(k,\omega)]^2+[\omega k^2D'(k,\omega)]^2}, \tag{E8}$$

where

$$\begin{aligned}D'(k,\omega)&=\frac{(\gamma-1)v_0^2}{S(k)}\frac{D_Tk^2}{\omega^2+(D_Tk^2)^2}\\&\quad+\psi_l(k,0)\frac{\tau_l(k)}{1+\omega^2\tau_l^2(k)},\\D''(k,\omega)&=-\frac{(\gamma-1)v_0^2}{S(k)}\frac{\omega}{\omega^2+(D_Tk^2)^2}\\&\quad-\psi_l(k,0)\frac{\omega\tau_l^2(k)}{1+\omega^2\tau_l^2(k)}.\end{aligned} \tag{E9}$$

To proceed with the numerical calculation, we need to know the details of the wave-number-dependent shear modulus $G_\infty(k)$ and the wave-number-dependent bulk modulus $K_\infty(k)$, which are related to the correlation functions of the stress tensor elements by

$$\begin{aligned}G_\infty(k)&=\beta\langle\sigma^{xy}_{-\mathbf{k}}\sigma^{xy}_{\mathbf{k}}\rangle,\\K_\infty(k)&=\frac{\beta}{3}[\langle\sigma^{zz}_{-\mathbf{k}}\sigma^{zz}_{\mathbf{k}}\rangle+\langle\sigma^{xx}_{-\mathbf{k}}\sigma^{zz}_{\mathbf{k}}\rangle].\end{aligned} \tag{E10}$$

The above-mentioned correlation functions are expressed in terms of the pair distribution function $g(r)$ and the pair potential $u(r)$ as

$$\begin{aligned}\langle\sigma^{zz}_{-\mathbf{k}}\sigma^{zz}_{\mathbf{k}}\rangle&=\frac{n}{\beta}\left[\frac{3}{\beta}+n\int d^3r g(r)\frac{\partial^2u}{\partial z^2}\left(\frac{1-\cos kz}{k^2}\right)\right],\\\langle\sigma^{xx}_{-\mathbf{k}}\sigma^{zz}_{\mathbf{k}}\rangle&=\frac{n}{\beta}\left[\frac{1}{\beta}+n\int d^3r g(r)\left(\frac{x}{z}\frac{\partial^2u}{\partial x\partial z}-\frac{x}{z^2}\frac{\partial u}{\partial x}\right)\right.\\&\quad\left.\times\frac{1-\cos kz}{k^2}\right],\\\langle\sigma^{xy}_{-\mathbf{k}}\sigma^{xy}_{\mathbf{k}}\rangle&=\frac{n}{\beta}\left[\frac{1}{\beta}+n\int d^3r g(r)\frac{\partial^2u}{\partial x^2}\left(\frac{1-\cos kz}{k^2}\right)\right],\end{aligned} \tag{E11}$$

where the pair distribution function $g(r)$ can be obtained using the Weeks–Chandler–Anderson method. Then given the Lennard-Jones potential

$$u(r)=4\epsilon\left(\frac{1}{(r/\sigma)^{12}}-\frac{1}{(r/\sigma)^6}\right), \tag{E12}$$

we are able to calculate all the necessary parameters for $J_l(k,\omega)$. The density correlation function $F(\mathbf{k},t)$ can be obtained with the following relations:

$$F(k,t)=\frac{1}{2\pi}\int_{-\infty}^{\infty}d\omega\, e^{i\omega t}S(k,\omega), \tag{E13}$$

$$S(k,\omega)=\frac{k^2}{\omega^2}J_l(k,\omega). \tag{E14}$$

The Lennard-Jones system of Xe liquid is equilibrated under reduced temperature $T^*=0.76$ and reduced density $\rho^*=0.85$ with parameters $\epsilon=236.6k_B$ and $\sigma=3.88$ Å. Under these parameters, the time unit for liquid Xe is $\sigma\sqrt{m/\epsilon}=2.7$ ps. The specific heat ratio is 1.87, the shear viscosity and bulk viscosity in reduced units are $\eta^*=24.0$ and $\eta_B^*=7.3$, respectively, which are taken from simulations under similar conditions in Ref. 65. To simplify the calculation, $D_T\approx0$ is assumed, i.e., the thermal diffusivity is neglected as an approximation. To proceed, the second frequency moment $\omega_l^2(k)$, the wave-number-dependent shear modulus $G_\infty(k)$, and the bulk modulus $K_\infty(k)$ are calculated with Eqs. (E5) and (E10); the wave-number-dependent relaxation time $\tau_l(k)$ is computed with Eq. (E6); the longitudinal current correlation function $J_l(k,\omega)$ in Eq. (E8) is calculated with the parameters obtained in the previous steps. Then, the density correlation function $S(k,\omega)$ can be calculated in the Fourier space, and its inverse Fourier transform of Eq. (E14) gives the intermediate scattering function $F(k,t)$.

[1] G. R. Fleming, *Chemical Applications of Ultrafast Spectroscopy* (Oxford, University Press London, 1986).
[2] S. Mukamel, *The Principles of Nonlinear Optical Spectroscopy* (Oxford, University Press, London, 1995).
[3] K. D. Rector, J. R. Engholm, J. R. Hill, D. J. Mayers, R. Hu, S. G. Boxer, D. D. Dlott, and M. D. Fayer, J. Phys. Chem. **102**, 331 (1998).
[4] P. Vohringer, D. C. Arnett, T.-S. Yang, and N. F. Scherer, Chem. Phys. Lett. **237**, 387 (1995).
[5] C. J. Brennan and K. A. Nelson, J. Chem. Phys. **107**, 9691 (1997).
[6] D. A. Blank, G. R. Fleming, M. Cho, and A. Tokmakoff, in *Ultrafast Infrared and Raman Spectrosopy*, edited by M. D. Fayer, 1999.
[7] P. Hamm, M. Lim, M. Asplund, and R. M. Hochstrasser, Chem. Phys. Lett. **301**, 167 (1999).
[8] R. F. Loring and S. Mukamel, J. Chem. Phys. **83**, 2116 (1985).
[9] Y. Tanimura and S. Mukamel, J. Chem. Phys. **99**, 9496 (1993).
[10] K. Tominaga and K. Yoshihara, Phys. Rev. Lett. **74**, 3061 (1995).
[11] T. Steffen and K. Duppen, Phys. Rev. Lett. **76**, 1224 (1996).
[12] T. Steffen and K. Duppen, J. Chem. Phys. **106**, 3854 (1997).
[13] D. J. Ulness, J. C. Kirkwood, and A. C. Albrecht, J. Chem. Phys. **108**, 3897 (1998).
[14] A. Tokmakoff, M. J. Lang, D. S. Larsen, G. R. Fleming, V. Chernyak, and S. Mukamel, Phys. Rev. Lett. **79**, 2702 (1997).
[15] W. Zhou and J. C. Wright, Phys. Rev. Lett. **84**, 1411 (2000).
[16] V. Astinov, K. J. Kubarych, C. J. Milne, and R. J. D. Miller, Chem. Phys. **327**, 334 (2000).
[17] O. Golonzka, N. Demirdoven, M. Khalil, and A. Tokmakoff, J. Chem. Phys. **113**, 9893 (2000).
[18] D. A. Blank, L. J. Kaufman, and G. R. Fleming, J. Chem. Phys. **113**, 771 (2000).
[19] L. Kaufman, D. A. Blank, and G. R. Fleming, J. Chem. Phys. **114**, 2312 (2001).
[20] J. Cao, J. Wu, and S. Yang, J. Chem. Phys. **116**, 3739 (2002), preceding paper.
[21] N. van Kampen, Phys. Norv. **5**, 271 (1971).
[22] J. A. Leegwater and S. Mukamel, J. Chem. Phys. **102**, 2365 (1995).
[23] S. Mukamel, V. Khidekel, and V. Chernyak, Phys. Rev. E **53**, R1 (1996).
[24] J. Wu and J. Cao, J. Chem. Phys. **115**, 5381 (2001).
[25] W. Miller, J. Chem. Phys. **54**, 5386 (1971).
[26] M. Ovchinnikov, V. A. Apkarian, and G. A. Voth, J. Chem. Phys. **114**, 7130 (2001).
[27] L. R. Pratt, Mol. Phys. **40**, 347 (1980).
[28] J. S. Hoye and G. Stell, J. Chem. Phys. **73**, 461 (1980).

[29] G. Stell, G. N. Patey, and J. S. Hoye, Adv. Chem. Phys. **48**, 183 (1981).
[30] D. Chandler, K. S. Schweizer, and P. G. Wolynes, Phys. Rev. Lett. **49**, 1100 (1982).
[31] R. M. Stratt, J. Chem. Phys. **80**, 5764 (1984).
[32] J. Cao and B. J. Berne, J. Chem. Phys. **99**, 6998 (1993).
[33] A. Tokmakoff, J. Chem. Phys. **105**, 1 (1996).
[34] A. Tokmakoff, J. Chem. Phys. **105**, 13 (1996).
[35] B. M. Ladanyi and S. Klein, J. Chem. Phys. **105**, 1552 (1996).
[36] J. T. Kindt and C. A. Schmuttenmaer, J. Chem. Phys. **106**, 4389 (1997).
[37] S. Saito and I. Ohmine, J. Chem. Phys. **108**, 240 (1998).
[38] R. L. Murry, J. T. Fourkas, and T. Keyes, J. Chem. Phys. **109**, 2814 (1998).
[39] R. L. Murry, J. T. Fourkas, W. Li, and T. Keyes, Phys. Rev. Lett. **83**, 3550 (1999).
[40] T. Keyes and J. T. Fourkas, J. Chem. Phys. **112**, 287 (2000).
[41] S. Mukamel, Annu. Rev. Phys. Chem. **51**, 691 (2000).
[42] K. Okumura and Y. Tanimura, J. Chem. Phys. **105**, 7294 (1996).
[43] Y. Tanimura, Chem. Phys. **2333**, 217 (1998).
[44] M. Cho, in *Advances in Multi-Photon Processes and Spectroscopy*, edited by S. H. Lin, A. A. Villaeys, and Y. Fujimura (World Scientific, Singapore, 1999).
[45] J. Y. Sung and M. Cho, J. Chem. Phys. **113**, 7072 (2000).
[46] H. Metiu, D. W. Oxtoby, and K. F. Freed, Phys. Rev. A **15**, 361 (1977).
[47] D. W. Oxtoby, Adv. Chem. Phys. **47**, 487 (1981).
[48] M. Maroncelli, J. MacInnis, and G. R. Fleming, Science **243**, 1674 (1989).
[49] J. S. Bader, B. J. Berne, E. Pollak, and P. Hanggi, J. Chem. Phys. **104**, 1111 (1996).
[50] B. J. Schwartz, E. R. Bittner, O. V. Prezhdo, and P. J. Rossky, J. Chem. Phys. **104**, 5942 (1996).
[51] S. A. Egorov and J. L. Skinner, Chem. Phys. **105**, 7047 (1996).
[52] B. J. Cherayil and M. D. Fayer, J. Chem. Phys. **107**, 7642 (1997).
[53] A. Ma and R. M. Stratt, Phys. Rev. Lett. **85**, 1004 (2000).
[54] T. I. C. Jansen, J. G. Snijders, and K. Duppen, J. Chem. Phys. **113**, 307 (2000).
[55] S. Mukamel, A. Piryatinski, and V. Chernyak, J. Chem. Phys. **110**, 1711 (1999).
[56] R. B. Williams and R. F. Loring, J. Chem. Phys. **110**, 10899 (1999).
[57] R. B. Willians and R. F. Loring, J. Chem. Phys. **113**, 10651 (2000).
[58] R. A. Denny and D. R. Reichman, Phys. Rev. E **63**, 065101 (2001).
[59] P. N. Butcher and D. Cotter, *The Elements of Nonlinear Optics* (Cambridge University Press, Cambridge, 1990).
[60] J. P. Boon and S. Yip, *Molecular Hydrodynamics* (McGraw–Hill, New York, 1980).
[61] J. P. Hansen and I. R. McDonald, *Theory of Simple Liquids* (Academic, New York, 1990).
[62] Y. X. Yan and K. A. Nelson, J. Chem. Phys. **87**, 6240 (1987); **87**, 6257 (1987).
[63] M. Berg, J. Phys. Chem. **102**, 17 (1998).
[64] A. Z. Akcasu and E. Daniels, Phys. Rev. A **2**, 962 (1970).
[65] D. Levesque and L. Verlet, Phys. Rev. A **7**, 1690 (1973).